2007

VGLUT and GAD65 Expression in Physiologically Characterized Ia Afferents

Ivonne Nkoli Ukpabi
Wright State University

VGLUT AND GAD65 EXPRESSION IN PHYSIOLOGICALLY CHARACTERIZED IA AFFERENTS

A thesis submitted in partial fulfillment

of the requirements for the degree of

Master of Science

By

IVONNE NKOLI UKPABI

B.S., University of Cincinnati, 2005

2007

Wright State University

WRIGHT STATE UNIVERSITY

SCHOOL OF GRADUATE STUDIES

October 31, 2007

I HEREBY RECOMMEND THAT THE THESIS PREPARED UNDER MY SUPERVISION BY Ivonne Nkoli Ukpabi ENTITLED VGLUT and GAD65 expression in physiologically characterized Ia afferents BE ACCEPTED IN PARTIAL FULFILLMENT OF THE REQUIREMENTS FOR THE DEGREE OF Master of Science.

Timothy Cope, Ph.D.
Thesis Advisor
Department Chair

Larry Ream, Ph.D.
Program Director

Committee on Final Examination

Timothy Cope, Ph.D.

Larry Ream, Ph.D.

Francisco Alvarez, Ph.D.

Joseph F. Thomas, Jr., Ph.D.
Dean, School of Graduate Studies

Abstract

Ukpabi, Ivonne Nkoli. M.S. Department of Neuroscience, Cell Biology and Physiology. Wright State University. 2007. VGLUT and GAD65 Expression in Physiologically Characterized Ia Afferents.

Peripheral nerve injury is known to induce several changes in the physiology and morphology of the injured afferent. These changes include hyperexcitability, decreased dorsal root potentials (DRP), loss of synaptic vesicles as well as loss of the vesicular glutamate transporter, VGLUT1. While many of the changes caused by peripheral injury revert with regeneration, others appear to be permanent. The loss of the stretch reflex for example is a puzzling outcome of recovery after peripheral nerve transection and regeneration, especially given that the electrical counterpart of the stretch reflex (the H-reflex) recovers after regeneration. We hypothesized that stretch induced transmission is suppressed at the primary afferent – motor neuron synapse and sought to determine whether this was due to a decrease in excitatory transmission or an increase in presynaptic inhibition. To this end, we measured the level of expression of VGLUT1 and 2 as well as the GABA synthesizing enzyme GAD65 in the central terminals of physiologically characterized primary afferents from healthy Wistar rats for comparison with regenerated animals. An inverse relationship appears to exist between VGLUT1 and GAD65 expression. Expression of the two proteins also differ in laminae V, VII and IX, with the highest VGLUT1 immunoreactivity in lamina V and the highest number of GAD65-intense presynaptic boutons in lamina IX. The possible effects of regeneration on this pattern are discussed.

Table of Contents

Introduction....1
Glutamate as an excitatory neurotransmitter....5
GABA as an inhibitory neurotransmitter....9
Hypothesis and Aims....11
Aim 1....12
Aim 2....13
Materials and Methods....15
Electrophysiological studies....15
Preparation of animals for recording....15
Data Collection....16
Tissue Preparation....17
Immunofluorescence....18
Confocal Microscopy....19
Results....21
Electrophysiological Results....21
Twitch response....21
Triangular Stretch and Release....22
Ramp-hold-release stretch....26
Vibrations....32
Regenerated Afferents....35
Immunohistochemical Results....36
Overall VGLUT1 Labeling....36
Overall VGLUT2 Labeling....41
Overall GAD65 Labeling....44
Labeled afferents: Physiology and Morphology....48
Discussion....53
Novel Findings....54
Physiology and relation to synaptic protein expression....56
Synaptic protein expression variations in different laminae....57
Bouton surface area as a measure of protein expression....58
Similarities along arborizations....60
Technical Limitations....63
Concluding Remarks....65
References....66

Introduction

The stretch reflex, also known as the deep tendon organ reflex, is the contraction of a muscle in response to a brief stretch of that muscle. This reflex is often initiated in a clinical setting by a light hammer tap on the tendon attached to the muscle of interest. The action potential generated by the stretch is transported to the spinal cord by Ia sensory afferents, which synapse directly onto α motor neurons located in the cord. An action potential at the motor neuron is transported back to the muscle, which results in the contraction of its extrafusal fibers.

Following nerve injury in the periphery, the axons near the injured area degenerate rapidly as the cell membrane and cytoplasm degrade in a process known as Wallerian degeneration (Waller, 1850; Beirowski et al, 2005). Degeneration in the proximal segment is proportional to the severity of the injury and generally extends to the next node of Ranvier, while the distal segment often degenerates up to the endplates. The resulting axonal debris is removed by Schwann cells and macrophages, leaving the neurolemma, the outermost cytoplasmic layer of Schwann cells, intact. The now hollow tube becomes instrumental in reinnervation of the target muscle. Attracted by growth factors released from the distal tube, the proximal segment of the injured nerve attempts to reattach to the distal portion.

Reinnervation is successful if a regenerating axon makes contact with the hollow tube located in the proximal segment, a process hastened by surgically attaching the two stumps together. Once in the tube, the axon is able to renew synaptic contacts within the empty gutters exposed by axonal degeneration. In the absence of a clear path to the distal portion, the regenerating axon may contact and innervate a separate muscle and the

hollow Schwann cell tube eventually shrinks over time.

Damage to peripheral nerves is well known to drastically alter the anatomy and neurochemistry of the injured afferents. For example, injury to C fibers and cutaneous Aβ fibers leads to an upregulation of neuropeptides such as vasoactive intestinal polypeptide and neuropeptide Y by the end of the first week (Wakisaka et al, 1991; 1992). Synaptic vesicles as well as synaptic contacts at the terminals of damaged afferents also gradually disappear during this period (Castro-Lopez et al, 1990).

Immunohistochemical studies by Hughes et al, 2004 showed that VGLUT1, one of the vesicular transporters that package the excitatory neurotransmitter glutamate into synaptic vesicles, decreased dramatically at synaptic terminals following axotomy of the sciatic nerve in rats. The decrease in VGLUT1 immunoreactivity was most visible in laminae III, IV, V and IX, where large cutaneous and proprioceptive afferents known to travel from the injured sciatic nerve terminate. The loss of synaptic vesicles may be the leading cause of the subsequent decline in VGLUT1. Alternatively, the dearth of VGLUT1 may lead to a decrease in synaptic vesicles, a situation observed by Fremeau et al 2004 in knockout mice lacking this transporter.

A number of physiological changes also take place following peripheral axotomy. For example, dorsal root potential (DRP) amplitudes decrease following axotomy of the sciatic nerve (Wall and Devor, 1981). The DRP is a prolonged depolarization at the central end of a dorsal root caused by action potentials traveling along neighboring roots (Barron and Matthews, 1938). This depolarization is used as a measure of presynaptic inhibition and is believed to cause either decreased neurotransmitter release or impulse transmission blockade (Wall and Lidierth, 1981). Axotomy also seems to trigger an increase in excitability as well as spontaneous firing (Devor and Seltzer, 1999). In

addition, after a brief high frequency electrical stimulation intended to facilitate synapses, the subsequent decrease in EPSP amplitude is much greater in chronically axotomized afferents than in healthy afferents (Mendell et al, 1995).

Following reinnervation of a muscle after peripheral nerve damage, the muscle afferents recover the ability to activate motor neurons, to modulate the tension of motor units and to respond to other reflexes (Cope and Clark, 1993; Cope et al, 1994). The animal regains significant use of the reinnervated muscle and motor axons appear to recover near normal functionality (Gordon and Stein, 1982; Gordon, 1987). However, studies have shown that the stretch reflex is lost. Not only is the reflexive contraction lost, stretching the muscle fails to modulate motor neuron responses to other afferents and pathways (Huyghues-Despointes et al, 2003; Cope and Clark, 1993; Cope et al, 1994).

Unlike motor axons, spindle afferents do not recover complete functionality after regeneration. Many regenerated muscle spindle afferents exhibit slower firing rates during ramp and static stretches. In general, however, most regenerated spindle afferents are capable of generating action potentials in response to stretch and some even recover enough to generate responses similar to their uninjured counterparts (Cope et al, 1994). Electrical stimulation of the damaged nerve evokes a normal sized EPSP, an indication that the circuit is perfectly capable of maintaining electrical and synaptic transmission (Haftel et al, 2005). The issue, therefore, remains why muscle stretch is incapable of initiating the reflex contraction present in healthy animals.

Given the wealth of information pointing to significant recovery of the circuit after nerve regeneration, we believe the suppression of stretch evoked action potentials occurs at the spindle afferent – motor neuron synapse. We hypothesized that morphological changes at the presynaptic terminal were responsible for the loss of the

stretch reflex. Such a disruption can be caused by two factors: an increase in presynaptic inhibition or a decrease in synaptic transmission at the central terminals of Ia afferents. To identify the cause, we studied the expression of the proteins directly responsible for presynaptic inhibition and synaptic excitation at the spindle afferent terminals of untreated animals for comparison with data from reinnervated animals. Glutamic acid decarboxylase, an enzyme responsible for synthesizing the inhibitory neurotransmitter GABA, and the vesicular glutamate transporters (VGLUT) 1 and 2 were chosen for their essential roles in inhibition and excitation, respectively.

A study such as this presents an opportunity to associate physiology with anatomy and function. Despite the veritable wealth of information available on the physiology and morphological makeup of Ia afferents, these two important halves have yet to be combined. Electrophysiological and immunochemical studies constantly espouse that slight variations exist between individual afferents from the same family. Studies on crustacean and frog neuromuscular junctions have shown that longer active zones promote greater synaptic release (Govind and Chiang, 1979; Atwood and Marin, 1983; Propst and Ko, 1987). Both physiological and morphological features of the neuromuscular junction can be modified by prolonged stimulation of the active zones. Other studies have documented increases in mitochondrial number and size, active zones and transmitter release following long term potentiation (Lnenicka et al, 1986; Chiang and Govind, 1986; Bailey and Chen, 1989). Such data on 1a afferents, on the other hand, are a lot less extensive. Part of this project aims to determine whether a relationship exists between VGLUT and GAD65 expression as well as between protein expression and Ia afferent physiology.

Glutamate as an excitatory neurotransmitter

Glutamate is an amino acid required by all cells to maintain their regular metabolism and protein synthesis. In the nervous system, glutamate serves as an excitatory neurotransmitter, the most abundant in excitatory synapses. Storage of glutamate at these synapses involves packaging of the amino acid into clear synaptic vesicles, a process that requires a high concentration gradient between the interior of the synaptic vesicle and the cytoplasmic space as well as between the cytoplasmic and extracellular spaces. Energy for neurotransmitter packaging is supplied by activation of H^+-ATPase by ATP, which creates a proton electrochemical gradient across the cell membrane.

All classical neurotransmitters rely on this gradient; however, different neurotransmitters utilize different components of the gradient. While transport of cationic transmitters like monoamines and acetylcholine (ACh) rely mostly on the transmembrane proton concentration gradient (ΔpH), glutamate transport primarily depends on the transmembrane electrical potential gradient ($\Delta\psi$) (Liu et al, 1997; Schuldiner et al, 1995). It may well be that this dependence on different components of the electrochemical gradient is necessitated by the state of the synaptic vesicles which contain the different neurotransmitters and that vesicles housing glutamate transporters are different from other synaptic vesicles (Fremeau et al, 2004). Glutamate transport occurs in vesicles where $\Delta\psi$ is greater than ΔpH, while ACh transport takes place in vesicles where the opposite is true. The presence of Cl^- channels in synaptic vesicles appears to play an important role in regulating the magnitude of these two components of the proton electrochemical gradient, as the entry of Cl^- ions leads to a decrease in $\Delta\psi$ and an

increase in ΔpH (Van Dyke, 1988; Forgac, 2000).

Two different classes of ion coupled glutamate transporters are responsible for creating and maintaining the electrochemical gradient. The first is a group of Na^+ coupled transporters located in the plasma membrane of the neuron. These excitatory amino acid transporters (EAAT 1- 5), along with astrocytes, are responsible for the reuptake of glutamate released into synaptic terminals (Chaudhry et al, 1995). Glutamine synthetase enzymes located in the astrocytes convert the reuptaken glutamate into glutamine, which is then transferred back to the neuron for reconversion to glutamate by the action of glutaminase (Rothstein and Tabakoff, 1984; Fremeau et al, 2004).

Beyond the plasma membrane, glutamate is packaged into synaptic vesicles by a class of H^+ coupled glutamate transporters located in the vesicular membrane. Transport of glutamate through these vesicular glutamate transporters (VGLUT 1-3) depends on the activation of vacuolar H^-ATPase to provide the energy necessary to create a H^+ electrochemical gradient across the membrane of the synaptic vesicle. Transport of the neurotransmitter is then achieved through an exchange with lumenal H^+ (Forgac, 2000; Johnson, 1988).

Despite cloning of the first vesicular glutamate transporter in 1994, the functional identity of the cloned protein, named BNPI for brain specific Na^+ dependent phosphate transporter, eluded researchers until 2000 (Ni et al, 1994; Otis, 2001). Genetic studies had revealed the role of *eat-4*, the *C elegans* homolog of BNPI, in glutamate release (Lee et al, 1999). The localization of the transporter at excitatory presynaptic terminals was also discovered using immunocytochemistry (Bellochio et al, 1998). BNPI was later renamed VGLUT1 after it was functionally identified by two different groups as a glutamate transporter (Bellochio et al, 2000; Takamori et al, 2000).

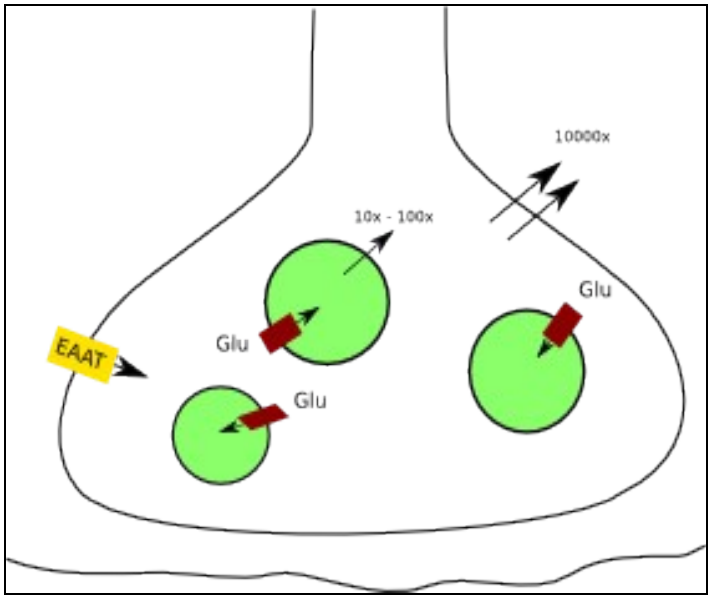

Fig 1. Glutamate transport requires a high concentration gradient between the extracellular and cytoplasmic spaces as well as between the cytoplasmic and intravesicular spaces. The concentration gradients are represented by arrows. Glutamate in the synapse is transported into the cytoplasmic space by the plasma membrane bound EAAT (excitatory amino acid transporter) while vesicular glutamate transporters (in red) package the glutamte into vesicles.

Since VGLUT1 is expressed by only a subset of glutamatergic neurons, the question remained whether there were other members of the VGLUT family yet to be discovered. A second vesicular glutamate transporter was identified soon afterwards, also masquerading as an inorganic phosphate transporter (Bai et al, 2001). The differentiation associated sodium dependent inorganic phosphate cotransporter (DNPI/VGLUT2) bore 82% similarity to VGLUT1 and was also localized exclusively at excitatory presynaptic terminals (Ni et al, 1994; Bai et al, 2001; Fremeau et al, 2001).

The third member of the family (VGLUT3), discovered a year later, has a 75% homology to its predecessors (Gras et al, 2002). Unlike the other two which rely on the presence of Na^+ ions, VGLUT3 is H+ dependent and possesses a higher affinity for glutamate. VGLUT3's dependence on the ΔpH component of the proton electrochemical gradient is also greater than that of the other VGLUTs.

Despite the existence of VGLUT3, VGLUTs 1 and 2 appear to be responsible for the majority of glutamate packaging in the adult brain (Bai et al, 2001; Fremeau et al,

2001). Expression of the two proteins follow a complementary pattern in the brain, with the neurons of the cerebral cortex, the hippocampus and the cerebellar cortex being the sole domain of VGLUT1, while the brain stem and the majority of the deep cerebellar nuclei express VGLUT2. VGLUT2 also predominates in the thalamus.

The two vesicular glutamate transporters VGLUTs 1 and 2 are known to undergo transcriptional regulation during development, with isotype switching from VGLUT2 to 1 occurring in the hippocampus, cerebellum and cortex of newborn rats. In the cerebellum, for instance, the dominant isotype in neonates, VGLUT2, is gradually down regulated over the first few weeks of development while VGLUT1 transcription is upregulated (Miyazaki et al, 2003). VGLUT1 becomes the primary isotype by day 30 with VGLUT2 left only in the climbing fibers. A similar trend has also been observed in the spinal cord of neonates (unpublished data from Alvarez lab).

The purpose of this isotype switch during development has yet to be determined. There is a possibility that the probability of release as well as the plasticity of the synapse may be related to the localized VGLUT subtype, with VGLUT1 expressed at synapses with a lower release probability and higher plasticity than VGLUT2 localizations (Hesler et al, 1993; Rosenmund et al, 1993; Dittman et al, 1998; Fremeau et al, 2004).

VGLUT3 expression in the brain is limited to specific cell populations, which accounts for its low density in the brain. The protein has been discovered at scattered excitatory interneurons in the cortex and hippocampus. These interneurons also express the GABA synthesizing enzyme GAD (Shaffer et al, 2002; Fremeau et al, 2002). Unlike the other VGLUTs, which are localized at synaptic terminals, VGLUT3 appears on both cell bodies and terminals. Expressed in the liver and the kidneys, VGLUT3 is also the only member of the family that appears outside the nervous system. The protein's

unpredictable expression patterns suggest it is utilized by cells that traditionally release a neurotransmitter other than glutamate (Fremeau et al, 2004).

The complementary distribution of the transporters in the brain generally matches their distribution in the spinal cord. VGLUT1 expression is mostly dominant in laminae III and IV as well as medial LV, indicating a localization in the central terminals of cutaneous and muscle mechanoreceptors (Alvarez et al, 2004). VGLUT2 on the other hand, is dispersed evenly throughout the grey matter but is strongest in LII and lateral LV (Varoqui et al, 2002). Other studies have reported that the majority of myelinated primary afferents express either VGLUT1, VGLUT2 or both in some cases, whereas nonmyelinated afferents either express neither transporter or express only VGLUT2 at low levels (Todd et al, 2003).

GABA as an inhibitory neurotransmitter

GABA (γ-aminobutyric acid) and glycine are the most common inhibitory neurotransmitters in the central nervous system (Devacel and van Den Pol, 1990). In the spinal cord, GABA fills the role of the major inhibitory neurotransmitter presynaptic to primary afferents in both the dorsal and ventral horns (Todd and Maxwell, 2000). For primary muscle spindle afferents, 91% of presynaptic inhibitory input in the ventral horn is provided by GABA-ergic boutons, while the remaining 9% of presynaptic boutons coexpress both GABA and glycine (Watson and Bazzaz, 2001). GABA-ergic boutons presynaptic to primary spindle afferents are slightly less in the dorsal horn, with only 51% of presynaptic boutons expressing only GABA and 31% expressing both GABA and glycine (Watson and Bazzaz, 2001). GABA-ergic inhibition is effected by the activation

of either $GABA_A$ receptors, $GABA_B$ receptors or both. $GABA_A$ receptor activation at synapses of primary sensory afferents causes depolarization and a decrease in excitability by changing the chloride conductance (Rudomin and Schmidt, 1999). $GABA_B$ receptor activation, on the other hand, does not affect the excitability of the terminal, but rather, reduces transmitter release by decreasing calcium influx (Quevedo et al, 1992; Edwards et al, 1989; Jimenez et al, 1991).

Synthesis of GABA requires glutamate as a precursor and is achieved by the action of the enzyme glutamic acid decarboxylase (GAD). Two isoforms of the enzyme, both capable of synthesizing GABA, have been discovered in the CNS and named after their molecular weights (Erlander and Tobin, 1991). Like VGLUTs 1 and 2 for glutamate, the presence of GAD65 and GAD67 can be used as a definitive marker of GABAergic synapses. The two isoforms retain a strong homology (> 95%) across all vertebrate species (Kaufman et al, 1986; Katarova et al, 1990). In the same species however, the amino acid sequences of the two proteins, their molecular weights (65 kDa and 67 kDa) and regulatory control differ considerably, which suggests two functionally different roles in the CNS (Kaufman et al, 1991; Esclapez et al, 1994).

Immunohistochemical studies by Kaufman et al, 1991 and Esclapez et al, 1994 identified the presence of the two GAD isoforms in both soma and axonal terminals in most regions of the brain. The two isoforms can form homodimers and heterodimers in soluble GAD (SGAD) and membrane associated GAD (MGAD) pools. GABA produced by the MGAD bound to synaptic vesicles is packaged into the vesicles by vesicular GABA transporters (Jin et al, 2003). In the spinal cord however, both isoforms are mostly localized to axonal boutons rather than cell bodies (Mackie et al, 2003). Both forms are present in the dorsal and ventral horns, but GAD67 is the dominant form in the ventral

horn. Laminae I-III contain the highest concentration of both proteins, while laminae IV-VI, lamina IX and the motor nuclei contain a moderate concentration. The concentrations of both isoforms are much lower in the remaining laminae (Feldblum et al, 1995; Mackie et al, 2003). Mackie et al 2003 also found that GAD67 immunoreactivity is relatively high in most of the laminae, while GAD65 has the highest density in laminae I, II and IX.

GAD65 immunoreactive boutons in lamina IX are generally arranged in clusters surrounding terminals that belong to Ia afferents (Hughes et al, 2005). These P boutons, as they are known, are presynaptic to Ia afferent boutons. The varicosities contacted by these boutons are also VGLUT1 immunoreactive. While GAD67 immunoreactivity in lamina IX is much greater than GAD65, P boutons contain little to no GAD67.

Hypothesis and Aims

Damage to peripheral nerves induces a host of physiological and neurochemical changes to circuits involving the injured nerves. Changes that occur with axotomy of spindle afferents include loss of synaptic contacts, synaptic vesicles and the vesicular glutamate transporter, VGLUT1. Dorsal root potentials as well as EPSPs elicited by electrical stimulation of transected afferents have been shown to decrease significantly in amplitude. During regeneration, transected axons can reattach to muscle and sensory receptors, leading to significant recovery of sensory encoding and muscle contraction. Electrical stimulation of regenerated spindle afferents succeeds at evoking EPSPs at axon-motor neuron synapse. This response is also known as the H-reflex. Stretching the muscle, however, fails to generate a synaptic response in the motor neuron, despite triggering action potentials in the sensory afferents.

We hypothesized that axotomy-induced morphological changes at spindle afferent synapses are responsible for the suppression of stretch evoked action potentials following regeneration. Suppression could be caused by failure to recover the VGLUT1 lost after axotomy. Such a situation would result in a decrease in synaptic excitation. Another possibility is an increase in presynaptic inhibition, a function carried out by GABA in spindle afferents. We present two aims to measure the levels of the vesicular glutamate transporters (VGLUT) 1 and 2, as well as the GABA synthesizing enzyme, GAD65, in healthy animals for comparison with animals that have undergone muscle reinnervation. In the course of the study, we plan to associate physiology with anatomy, notably using immunohistochemistry, in an attempt to identify relationships between the two.

Aim 1

Primary spindle afferents, also known as Ia afferents, are one of the two types of afferents innervating the muscle spindle, a stretch receptor responsible for transducing the mechanical stimulation into electrical signals (i.e. action potentials). The electrical signals are then transmitted to the spinal cord by the primary and secondary afferents innervating the spindle's intrafusal fibers. Group Ia afferents are large diameter afferents with high conduction velocities, whereas the secondary spindle afferents (group II) have smaller diameters and conduction velocities. The two afferent types possess different physiological properties and therefore exhibit different responses to muscle stretch. Ia afferents are sensitive to changes in muscle length (static sensitivity) as well as the velocity of the length change (dynamic sensitivity). Group II afferents, on the other hand, possess only static sensitivity (Matthews 1963; Cheney and Preston, 1976a, b; McCloskey, 1978).

Characteristics of Ia afferents are well known. Electrical stimulation of a healthy muscle results in reflex contraction known as the isometric twitch. Muscle spindle afferents (both group Ia and II) discharge initially, but are inhibited during muscle contraction. Other characteristic behaviors of Ia afferents can be identified by applying stretch to the innervated muscle. For example, linear stretch of the muscle results in an initial burst of high frequency firing, which disappears after a few spikes (Haftel et al, 2004). Ia afferents are also known to react specifically to sinusoidal vibrations at low amplitudes (DeDoncker et al, 2003).

The first goal of this project is to study the physiological and morphological properties of uninjured afferents in order to have a reliable source of comparison with regenerated afferents. Afferents used for the study must exhibit the characteristics mentioned above to be considered healthy. Utilizing a number of different electrophysiological tests allows us to observe afferents' responses to electrical stimulation as well as to muscle stretch. We can then visualize the axon's morphology in the spinal cord by filling it with the dye tracer neurobiotin.

Aim 2

Within the cord, primary spindle afferents bifurcate multiple times to form a dense network of contacts throughout the intermediate and ventral horn regions (Brown and Fyffe 1978). Contacts in the intermediate region (Rexed's laminae V and VI) are often in the form of en passant associations with numerous interneurons. This region contains the most complex arborizations and a high concentration of synaptic contacts with non-antagonistic neurons involved in non-reciprocal Ia inhibition. Further branching occurs in laminae VII and IX, ventrolateral to the intermediate region. Contacts in lamina

VII are simpler associations between Ia afferents and interneurons implicated in the Ia reciprocal inhibitory pathway (Jankowska and Lindstrom, 1972). Interneurons located in this lamina are modulated by antagonistic neurons. Excitatory contacts between the Ia afferent and corresponding motor neuron occurs in lamina IX.

Filling the axon with a dye tracer allows us to pair physiological properties with the morphology of the axon. Not only can we confirm the axonal identity implied by physiological responses, we are able to examine in depth synapses belonging to selected afferents. The second part of this project involves measuring the expression of proteins involved in synaptic excitation and presynaptic inhibition along central terminals of Ia afferents in laminae V, VII and IX. The rationale for measuring protein expression in the different laminae is that we believe CNS-mediated suppression of transmission occurs in these terminals following peripheral nerve transection, which leads to the loss of the stretch reflex after regeneration. This suppression can be accomplished by either increasing GABA mediated presynaptic inhibition or decreasing glutamate mediated synaptic excitation. Measuring the expression of the GABA synthesizing enzyme GAD as well as the vesicular glutamate transporters 1 and 2 in healthy animals will allow us to pinpoint changes following regeneration.

Materials and Methods

Electrophysiological studies

Preparation of animals for recording

All procedures used in this study complied with the standards of the Wright State University Institution of Animal Care and Use Committee (IACUC). A total of 17 female Wistar rats were used, including 14 controls and 3 animals with transected and subsequently regenerated medial gastrocnemius nerves. The rats were deeply anesthetized in an induction chamber filled with 5% isoflurane (Fischer). Anesthesia was maintained over the course of the experiment by continuous delivery of 1-3% isoflurane through a tube inserted into the trachea by retrograde intubation. The rectal temperature was maintained at approximately 37°C using a heating pad and lamp. The heart rate, respiratory rate and CO_2 were also monitored and maintained within normal levels.

The animals underwent surgery to expose the lateral and medial gastrocnemius and isolate the complementary nerves. All other nerves in the surrounding area (post tibial, common peroneal and sural) were either cut or crushed. The tendon of the triceps surae muscle was cut at the insertion point and tied to a lever attached to an Aurora Scientific motor which was used to apply stretch to the muscle. The resting length of the LG was determined by tying a suture to the end of the muscle and aligning it with another suture tied to the plantaris muscle. The flap of skin surrounding the area was used to form a pool filled with mineral oil (Fischer). Both the MG and LG nerves were placed on the same bipolar electrode and electrical stimulation was applied to the nerves from an isoflex (A.M.P.I.).

The spine of the rat was suspended in a stereotaxic frame and a laminectomy performed to expose the spinal cord. A mineral oil pool was also created at this site using the skin around the incision.

Data Collection

The dorsal root with the highest activity following a stretch of the LG or MG was selected and placed on bipolar electrodes for study. Glass micropipettes with a ~1 μm tip filled with 4% neurobiotin in 0.3M NaCl were used to obtain intracellular recordings from 1a afferents. Intracellular records were obtained by propelling the micropipette into the selected dorsal root in 2 μm steps using a microstepper. Recordings were taken from afferents that exhibited action potentials in response to electrical stimulation of the LG and MG nerves as well as stretching of the corresponding muscles. Preliminary characterizations of the afferents were based on their behavior during twitch contraction. Firing at the beginning of the contraction followed by an inhibition at the peak of contraction identified the afferent as a spindle afferent. With no distinction made between Ia and group II spindle afferents at this point, further tests were used to identify afferent type.

Following preliminary characterization, the afferent's firing response to muscle stretch was analyzed by applying various stretch patterns. These included triangular stretch and release trials, ramp-hold-release trials, as well as vibrations at different frequencies. The stretch and release trials were applied as a set of three consecutive triangular stretches, each with an amplitude of 3 mm and a velocity of 4 mm/s. The ramp and hold stretches also had an amplitude of 3 mm and the hold phase ranged from 0.2 –

5s. Vibrations with amplitudes of 0.08 mm and frequencies ranging from 20-167 Hz were also applied to the muscle and the resultant response recorded. Collection and analysis of the data was performed using Spike2 software (ver. 5.15).

Tissue Preparation

After successful characterization, neurobiotin was injected into the afferent by applying a continuous pulse of current (5 nA to 14 nA) for a period of 8 – 25 minutes. To optimize the transport of neurobiotin from the injection site in the dorsal root to the afferent's terminations in the spinal cord, anesthesia was maintained for at least another 6 hours before transcardial perfusion using 4% paraformaldehyde (PFA) in 0.1 M phosphate buffer (PB). The spinal cord was harvested and postfixed in a solution containing 4% PFA, 0.1M PB and 7.5% sucrose. The postfixation period varied from 8 hrs to 3 days depending on the effectiveness of the perfusion. One of the animals expired exactly 5 hrs after the neurobiotin fill and the tissue required a longer post fixation than the rest. Despite the long post fixation, the tissue harvested from this animal remained fragile.

After postfixation, the harvested spinal cord was placed in a vial containing 15% sucrose, 0.1 M PB and 0.01% sodium azide for cryoprotection and allowed to incubate overnight before processing. A block of tissue between the L3 and S1 segments of the cord was cut on a freezing sliding microtome at a thickness of 50 μm (or 100 μm for very soft tissue) and the cross sections were collected serially in vials containing 0.1 M PBS. Cryoprotection during cutting was achieved by surrounding the tissue block with a liberal amount of Optimal Cutting Temperature gel (O.C.T).

Immunofluorescence

All washes were done in 0.1 M PBS (3 washes, five minutes each) and processing was done "free-floating". All antibodies, primary and secondary, were diluted with 0.1M PBS with 0.03% Triton and incubations were done on an orbital shaker at room temperature. A comprehensive list of antibodies is presented in **Table 1**. After cutting, the tissue sections were first washed to remove any residual O.C.T, then incubated overnight in streptavidin conjugated to FITC (Jackson, 1:1000). Once the antibody was washed off, two sections were taken from each vial and studied under the microscope.

Vials containing sections with intracellularly stained Ia afferent collaterals were used for subsequent steps and all others discarded. The sections were placed in a solution containing 4% PFA and 0.1M PB for 5 minutes to prevent washing out of fluorochrome-conjugated streptavidin during further processing. After another wash, the sections were incubated for an hour in normal donkey serum (1:10 in 0.1M PBS with 0.1% Triton). The sections in each vial were split into three groups and incubated overnight in the following three primary antibodies: VGLUT1 (1:5000, Synaptic Systems, rabbit polyclonal), VGLUT2 (1:1000, Synaptic Systems, rabbit polyclonal) and GAD65 (1:400, PharMingen, mouse). Following a wash the next day, a 2 hr incubation in Cy3-conjugated (1:50, Jackson) anti rabbit or anti mouse antisera depending on the primary antibody - was used to reveal the immunoreactive sites. The sections were then washed, mounted on slides and coverslipped with Vectashield (Vector) for further study.

Table 1. Antibodies used for immnunohistochemistry

Antibody	Dilution	Species	Source
Streptavidin FITC	1:100		Jackson IR
VGLUT1	1:5000	Rabbit Polyclonal	Synaptic Systems
VGLUT2	1:1000	Rabbit Polyclonal	Synaptic Systems
GAD65	1:400	Mouse Monoclonal	PharMingen
Cy3	1:50	Donkey	Jackson IR

Confocal Microscopy

Confocal images were acquired with an Olympus Fluoview FX using lasers with excitation lines of 488 and 568 nm. In the interest of normalizing the final results, acquisition parameters were maintained at a set value across all images used for intensity analysis. Images from the contralateral sides of the spinal cord cross sections were used as controls and to confirm background intensities. Data collection was done with the Fluoview FV300 software while a newer version of the software (Fluoview FV500) was used for analysis. Figures were created using OpenOffice Draw and Inkscape with manipulation of images limited to adjusting brightness and contrast for better clarity. Statistical analysis was performed with Statistica and OpenOffice Calc.

To identify the morphology of the filled afferents, low resolution (10X) confocal images were taken of each spinal cord cross section. Higher resolution images (60X) of the afferents were obtained and approximately 50 boutons randomly picked from laminae V, VII and IX for study. A total of ~450 boutons (150 boutons per antibody) were studied for each animal unless otherwise stated. Bouton boundaries were traced using Fluoview FV500 and the analysis component of the software was used to calculate the average surface areas and intensities of the selected boutons. To determine the extent

of antibody penetration, the position of each bouton within the Z stack was noted. Bouton intensities were normalized across all afferents by subtracting the background intensity for each bouton, a value obtained by measuring the intensity of the selected bouton at a different Z position devoid of antibody or neurobiotin labeling.

Results

Electrophysiological Results

Twitch response

Conduction velocities of the afferents were not calculated, therefore, a combination of electrophysiology and afferent morphology was used to confirm that they were indeed Ia afferents. Orthodromic action potentials from each impaled afferent were recorded following electrical stimulation at one pulse per second. Of the 24 control afferents studied, 19 discharged at the onset, then paused during muscle contraction following the stimulus (**Fig 2**). The remaining five fired during the peak of muscle contraction, a response attributed to afferents innervating Golgi tendon organs, also known as group Ib afferents (**Fig 2d**). To avoid confusion, these afferents will only be referred to as Golgi tendon organ afferents henceforth.

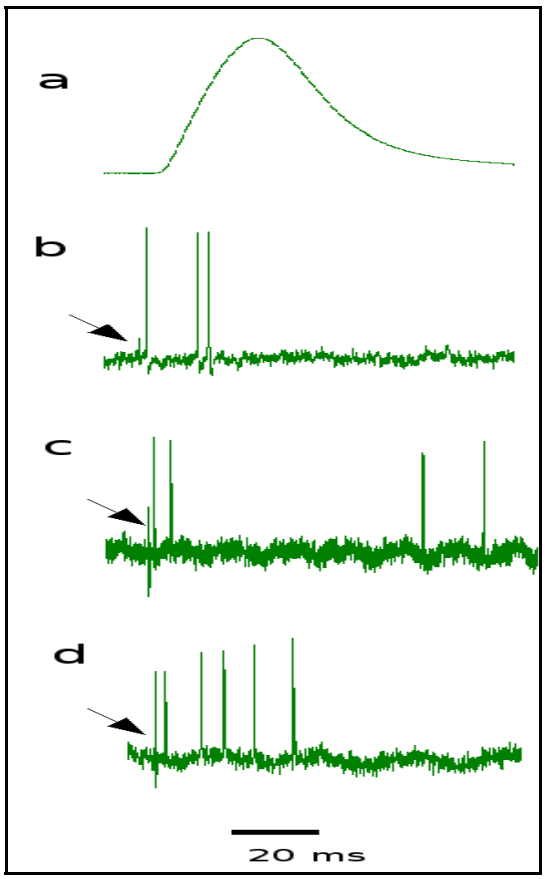

Fig 2. Afferent firing observed in response to electrical stimulus. **a** represents muscle contraction. **b** and **c** are representative of spindle afferents while **d** is a typical response from a golgi tendon afferent. Arrows indicate stimulus artifacts.

Pausing during contraction is a universal response in spindle afferents, as tension imposed on the muscle spindle by the slightest stretch is alleviated during contraction. Of the 19 identified spindle afferents, a majority (16) resumed firing after contraction (**Fig 2c**). Using this criterion, each afferent was easily classified as either a spindle or a Golgi tendon organ afferent.

Triangular Stretch and Release

Instantaneous firing rates from each afferent were recorded during a series of three consecutive triangular stretches. For similar stretches while recording from afferents, Haftel et al, 2004 reported a higher instantaneous firing rate (IFR) or dynamic response (DR) during the rising phase of the first stretch when compared to the other two. The dynamic response in subsequent stretches remained depressed unless an interval was allowed between stretches and is indicative of a history dependence. Haftel observed that the longer the interval, the greater the recovery of the afferent, with 120 seconds being the minimum period needed for full recovery. In many spindle afferents, the first triangular stretch also elicited an initial burst comprised of a few (less than 4) spikes that was absent in subsequent stretches applied without an interval.

Of the 19 afferents with typical spindle afferent twitch responses, 15 exhibited an initial burst (**Fig 3b, c**), which was absent in all 5 afferents classified as golgi tendon organ afferents (**Fig 3a**). The history dependence of the two afferent types is represented in **Fig 4** where the instantaneous firing rate is plotted against the length of the muscle during stretch. In contrast to spindle afferents (**Fig 4a**), tendon organ afferent firing rates are less affected by previous movement (**Fig 4b**). These afferents tend to have fewer

spikes and a lower peak firing rate, a value that is generally higher for the first triangle in both types of afferents. The average number of spikes produced by spindle afferents is 59 (± 19 SD), 41 (± 14 SD) and 38 (± 14 SD) for the first, second and third triangles respectively. Tendon organ afferents on the other hand, produce 32 (± 15 SD), 26 (± 15 SD) and 23 (± 15 SD) spikes on average for the same triangles. The IFR drop, the difference between the peaks of the rising and falling phases, is also much lower for tendon afferents. Qualitative comparisons between the triangles are presented in **Table 2** for spindle and tendon organ afferents.

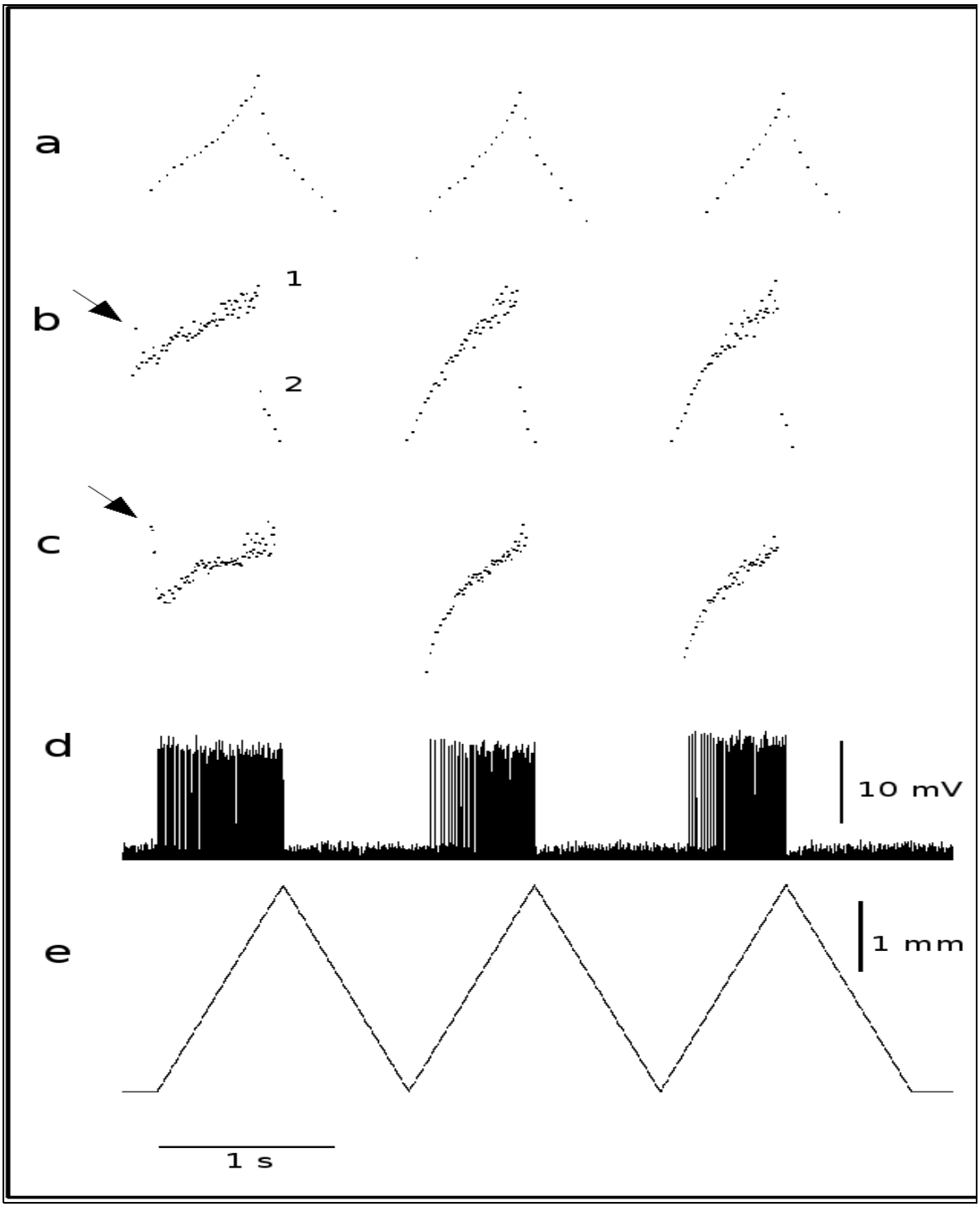

Fig 3. Responses to triangular stretch from afferents innervating golgi tendon organs (**a**) and muscle spindles (**b**, **c**). The IFR drop is the difference between the peak firing rates during the height of the rising phase (1) and the beginning of the falling phase of the triangle (2). Arrows point to initial burst peaks.

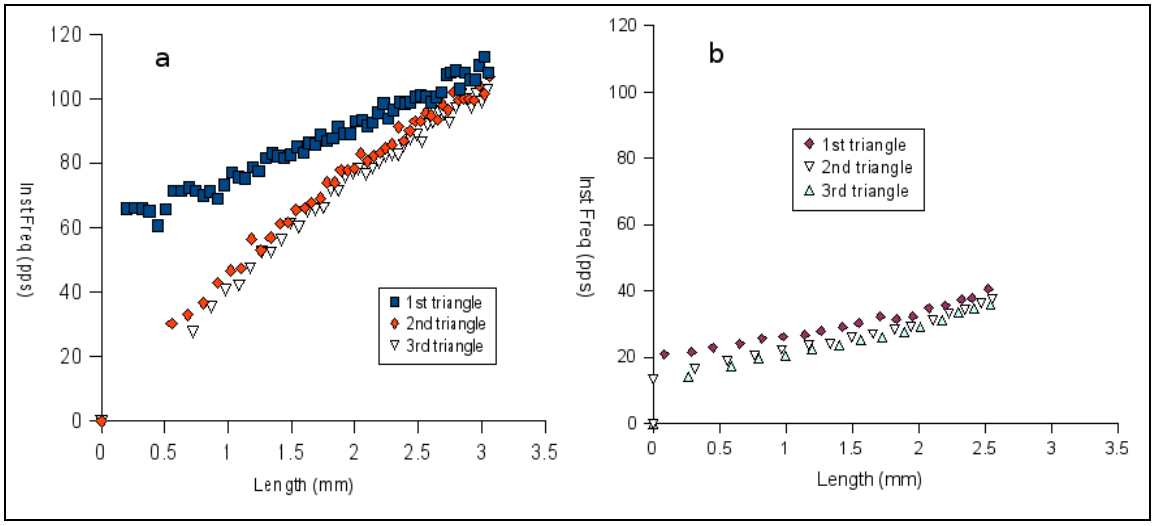

Fig 4. Dynamic response during three consecutive triangular stretches with 3 mm amplitudes. In a plot of instantaneous frequency over muscle length, spindle afferents (**a**) are easily distinguishable from afferents innervating golgi tendon organs (**b**) due to their steep slopes, higher firing rates and history dependence.

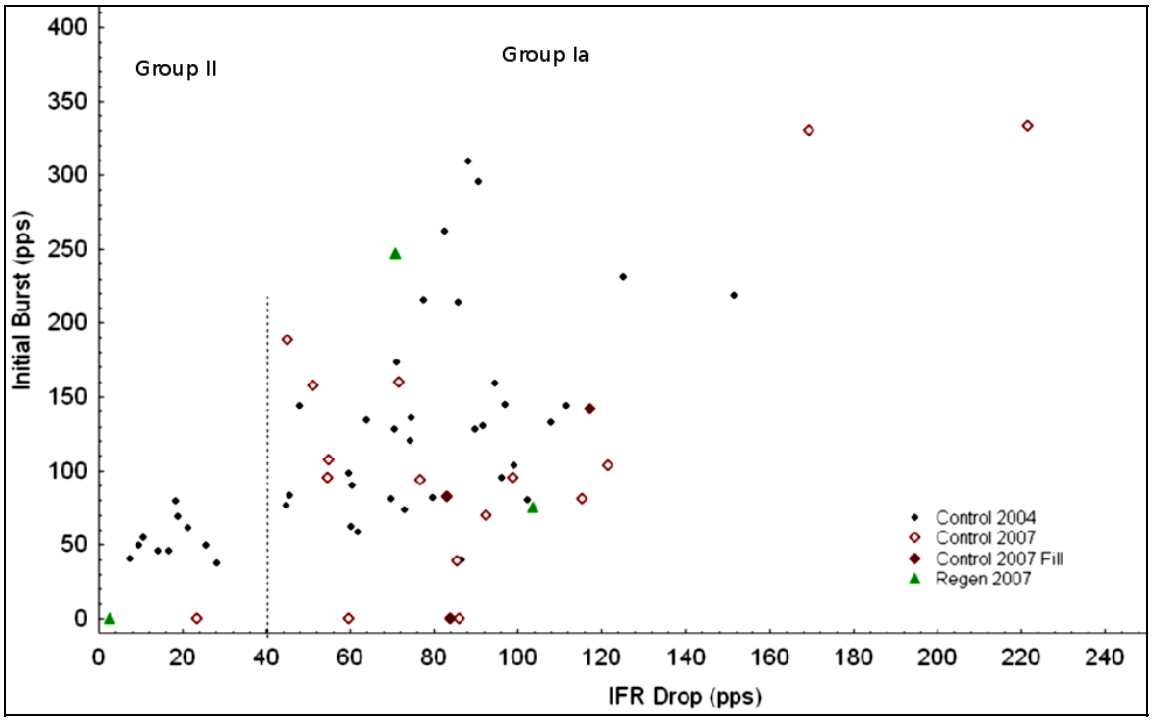

Fig 5. Initial burst vs IFR drop during the first trial of three consecutive triangular stretches applied to spindle afferents. Data collected by Haftel (1999) (n = 49) is shown here for comparison with our most recent control data (n = 16), control afferents filled with neurobiotin (n = 3) and regenerated afferents (n = 3). IFR drops below 40 pps are believed to be characteristic of group II afferents. Afferents lacking initial bursts are marked by initial burst values of 0.

a

n = 19		Average	StDev	Max	Min
IB	1st Triangle	154.29	85.86	505.05	29.47
Slope	1st Triangle	24.8	12.41	59.9	2.72
	2nd Triangle	38.57	14.94	73.35	15.97
	3rd Triangle	39.75	15.92	77.17	14.07
Spikes	1st Triangle	59.48	19.57	122	24
	2nd Triangle	41.09	14.43	94	14
	3rd Triangle	38.37	13.94	91	12
IFR Drop	1st Triangle	93.76	42.18	227.77	23.43
	2nd Triangle	94.96	45.19	221.55	19.87
	3rd Triangle	95.86	45.78	231.48	7.67
IFR Max	1st Triangle	121.3	38.15	234.74	60.98
	2nd Triangle	117.84	37.65	231.48	56.5
	3rd Triangle	115.28	37.36	231.48	58.48

b

n = 5		Average	Stdev	Max	Min
Slope	1st Triangle	15.38	8.58	41.47	7.13
	2nd Triangle	20.63	14.22	60.37	8.01
	3rd Triangle	21.57	15.14	61.7	9.24
Spikes	1st Triangle	32.96	14.86	71	10
	2nd Triangle	26.13	15.48	73	6
	3rd Triangle	23.83	15.09	69	6
IFR Drop	1st Triangle	15.74	6.9	30.02	1.95
	2nd Triangle	15.25	7.28	29.51	2.94
	3rd Triangle	14.4	7.49	29.13	4.95
IFR Max	1st Triangle	61.81	34.65	157.83	31.21
	2nd Triangle	59.61	36.25	162.76	29.98
	3rd Triangle	58.2	35.87	160.26	28.06

Table 2. Numbers represent spikes per second. Qualitative comparison of spindle afferents (**a**) against tendon organ afferents (**b**) in response to three triangular stretch illuminates numerous differences between the two. Spindle afferents possess initial bursts (IB), steeper firing rate vs muscle length slopes, greater IFR drops and also higher maximum IFR.

IFR drops of the spindle afferents studied were split into two groups. The majority of the spindle afferents had IFR drops above 40 pps and only two afferents (one non-filled control, one regenerated) were significantly below 40 pps. All these afferents could be characterized as spindle afferents due to their isometric twitch responses, therefore the lower IFR drop could be an indication of a different afferent type. In fact, Haftel (1999) had characterized afferents with IFR drops below 40 pps as group II spindle afferents. Data collected by Haftel (1999) are presented in **Fig 5** for comparison.

Ramp-hold-release stretch

Ramp-hold-release stretches with an amplitude of 3 mm and various durations were applied to the gastrocnemius muscle while recording from innervating afferents. Three different durations were used; all had a ramp phase lasting 0.15 s and hold phases

ranging from 0.2, 0.5 and 1s. The ramp was released over a time period of 0.15 s.

The responses to these series of stretches bore few similarities to the preceding triangular stretch and release trials. Tendon organ afferents again demonstrated a lack of an initial burst (**Fig 6**) as well as lower spike counts and peak firing rates. Stretches were generally applied as series of three consecutive trials followed by a rest period of 4s. In contrast to the response during stretch and release trials, the dynamic response changed little between the first and third ramp in spindle afferents (**Fig 7**). Initial bursts were also observed at the beginning of each ramp and hold trial. Stretches that involved more than three consecutive trials also showed little change between the first and last trials.

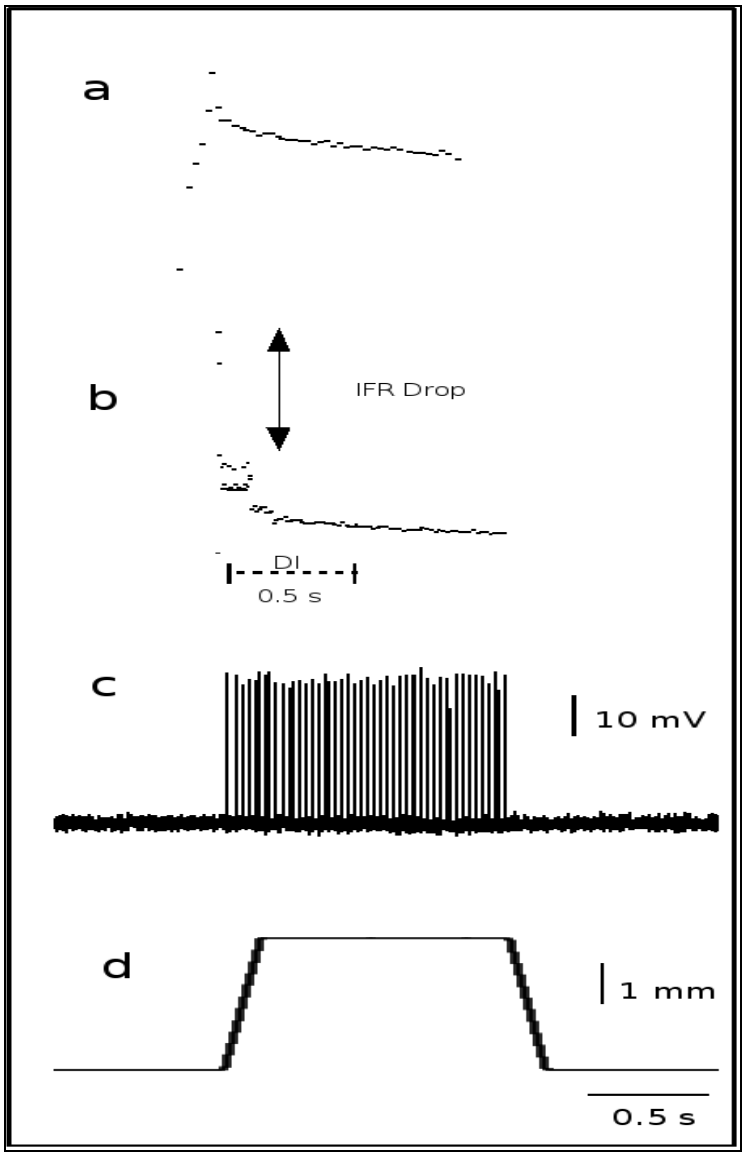

Fig 6. Afferent responses to ramp and hold stretch. Tendon organ afferents (**a**) lack the drop in firing rate between the peak of the ramp and the beginning of the hold phase, a behavior generally found in spindle afferents (**b**). The dynamic index (DI) is measured as the difference between the maximum firing rate at the end of the ramp phase and the firing rate 0.5s later during the hold phase.

Dynamic indices (DI) were calculated as the difference between the peak firing rate during the end of the rising phase and the firing rate of the afferent 0.5 seconds later regardless of total hold time (Matthews 1963, Crowe and Matthews 1964). Average DI was 100 ± 48 pps (SD) and DI could not be determined for trials with hold times less than 0.5 seconds. A linear correlation exists between the dynamic index and the IFR drop for these series of stretches as shown in **Fig 7**, with the DI being an average of 14 ± 16 pps (SD) higher than the IFR drop. Unlike with stretch and release trials, the IFR drop for ramp and hold stretches measures deceleration of the firing rate over a fixed length, which is similar to the DI.

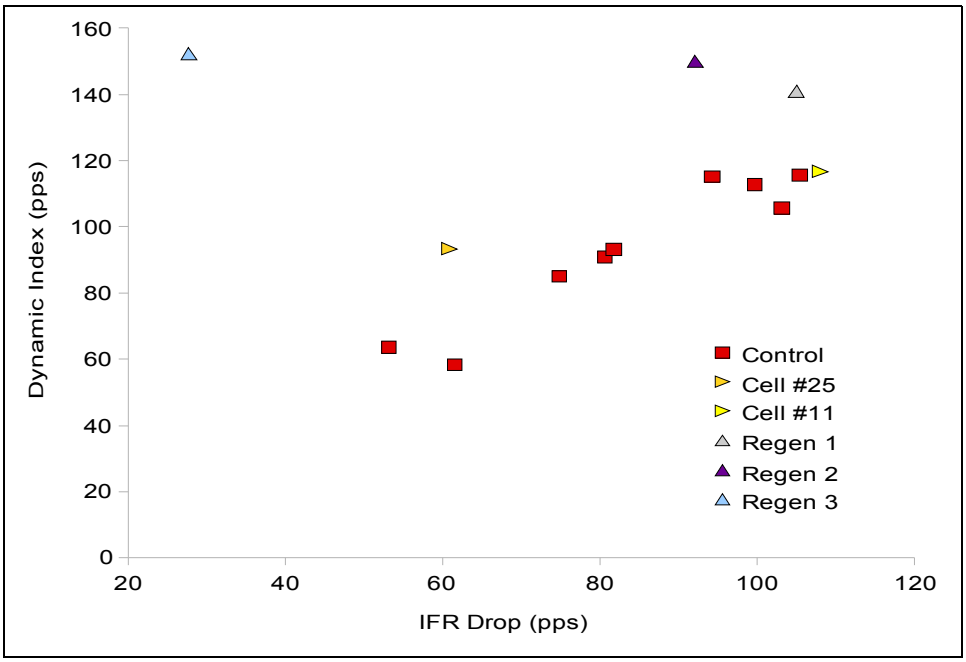

Fig 7. Dynamic indices (DI) vs IFR drops of one ramp and hold stretch trials. The duration of the ramp phase is 0.15 s with a hold phase of 1 s followed by a release lasting 1.5 s. A linear relationship exists between DI and IFR drop in control afferents. DI was not calculated for afferents that received stretches with less than 0.5s hold, therefore those afferents as well as those without IFR drops are excluded. Cells 11 and 25 correspond to two out of the three neurobiotin labeled afferents.

For 3 mm/s stretches with a hold period of 5s applied to muscles while recording from spindle afferents, De-Doncker et al 2003 identified two types of responses. Ia afferents possessed a high peak firing rate at the end of the ramp phase (125 ± 6.7 SD pps) while the peak firing rate of group II afferents was much lower (63 ± 3.5 SD pps). De-Doncker, 2003 also observed that Ia afferents had a higher dynamic index than group II afferents. For our studies, the one suspected group II afferent regrettably received only stretches with 0.2 s hold times, which was too short to calculate the dynamic index. The average peak IFR for afferents that received a similar stretch, however, was 184 ± 91 pps (SD), with that particular afferent trailing the group at 107 ± 10 pps (SD).

DI values have been shown to increase with stretch velocity, stretch amplitude and muscle length (Houk et al 1981, Matthews 1963, 1972). Comparison between different stretch durations applied to the same afferent shows a linear decrease in both DI and the peak firing rate at the end of the ramp as the duration of the stretch was increased. With a consistent amplitude of 3 mm and a resting length normalized to take into account variations in each animal, stretch velocity was the primary determinant of the maximum IFR, the IFR drop and the DI. **Figure 8** shows the change in IFR max and DI in two different cells as ramp and hold stretches with various durations were applied. Increasing the hold period while maintaining a constant rise duration causes an increase in the slope and number of spikes during the hold phase (**Table 3**). In contrast, the maximum and minimum firing rates during the hold decrease, though they appear similar in hold periods of 0.5 and 1.0 s.

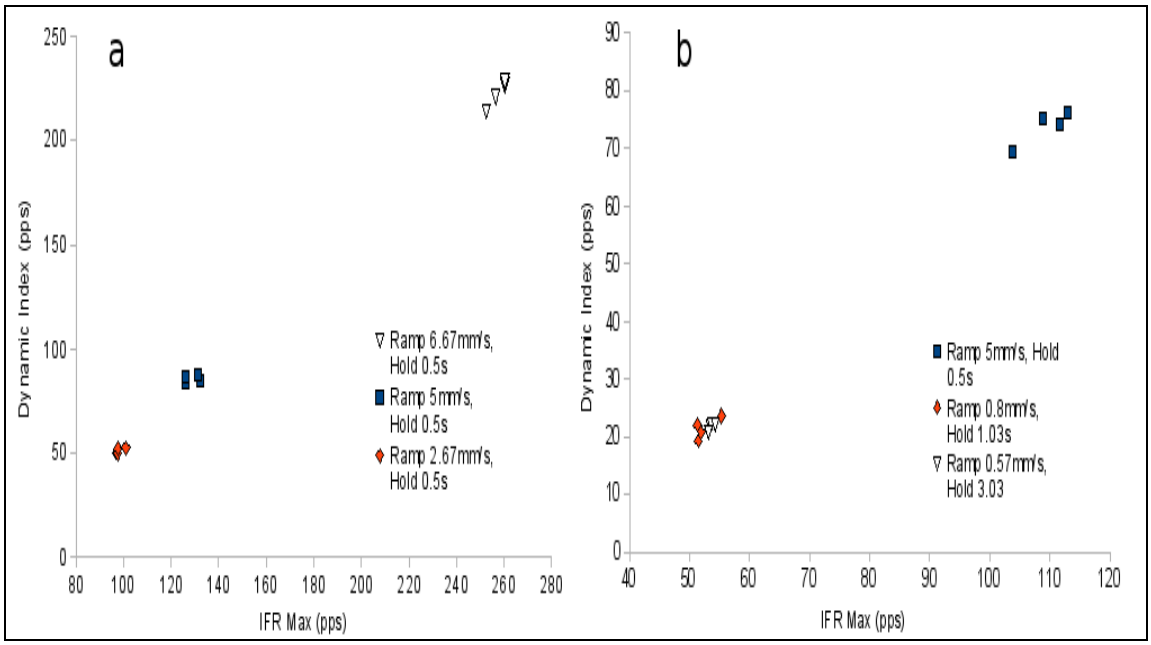

Fig 8. The velocity of the ramp phase of a ramp-hold-release stretch determines both the maximum firing rate and the DI of an afferent. The greater the stretch velocity, the higher the values of the DI and maximum firing rate. A single afferent's responses to stretches with increasing velocity and a consistent hold duration is shown in **a**. Responses of three different afferents are shown in **b**.

		Ramp Total (s) / Hold (s)				Ramp Total (s) / Hold (s)				Ramp Total (s) / Hold (s)			
		0.5 / 0.2				0.8 / 0.5				1.3 / 1			
		Average	StDev	Max	Min	Average	StDev	Max	Min	Average	StDev	Max	Min
IB	1st Ramp	423.69	92.51	537.63	273.22	428.32	33.18	462.96	396.83	327.95	145.82	476.19	74.4
	2nd Ramp	411.66	73.62	476.19	268.82	439.05	57.9	505.05	396.83	351.16	122.62	476.19	68.08
	3rd Ramp	399.34	76.11	469.92	264.55	434.1	49.45	490.2	396.83	369.59	128.24	476.19	63.52
Slope Rise	1st Ramp	33.38	23.48	75.13	5.15	26.24	24.05	69.84	3.02	34.26	16.89	77.68	8.58
	2nd Ramp	35.68	20.03	72.33	14.84	32.84	23.63	73.36	9.46	44.51	19.85	86.95	10.88
	3rd Ramp	33.45	19.33	81.29	14.79	34.7	24.48	78.4	10.75	43.41	21.37	89.43	15.83
Slope Hold	1st Ramp	-84.12	42.62	-13.53	-147.75	-41.55	17.38	-30.92	-76.03	-24.58	7.03	-10.55	-35.95
	2nd Ramp	-88.69	43.75	-26.64	-161.4	-44.4	13.65	-31.67	-70.96	-23.51	6.68	-6.98	-35.72
	3rd Ramp	-85.43	48	-14.71	-185.1	-39.62	13.65	-31.11	-65.67	-22.91	7	-6.66	-36.76
Spikes Rise	1st Ramp	21.14	6.71	31	15	17.33	4.79	27	14	18.26	3.45	21	15
	2nd Ramp	20.76	6.52	31	14	16.17	4.69	26	13	16.7	3.5	22	12
	3rd Ramp	20.05	6.8	31	14	16	5.74	28	12	16.74	3.97	23	11
Spikes Hold	1st Ramp	16.76	6.23	27	9	27.83	10.26	47	18	57.11	16.36	107	30
	2nd Ramp	16.57	6.02	26	8	26.67	10.41	46	17	55.26	16.78	106	29
	3rd Ramp	15.89	6.35	26	7	26	9.25	43	17	56.65	16.98	104	30
Hold Max	1st Ramp	99.67	40.93	168.46	52.21	69.62	24.96	118.2	49.88	75.57	16.86	117.7	43.67
	2nd Ramp	98.98	38.25	165.34	50.59	66.81	24.26	112.61	44.42	76.15	19.57	127.03	42.92
	3rd Ramp	94.18	39.38	168.46	42.62	67.63	22.02	108.93	45.91	73.74	19.42	120.42	41.24
Hold Min	1st Ramp	73.06	32.91	124.88	16.94	47.6	17.14	77.88	30.79	43.82	16.88	87.17	19.35
	2nd Ramp	74.48	30.37	125.75	32.89	44.98	16.79	76.8	29.47	43.36	17.73	94.27	11.42
	3rd Ramp	72.36	30.73	121.48	32.43	45.79	17.23	77.88	29.86	44.93	17.92	95.57	10.9
DI	1st Ramp	-	-	-	-	94.96	41.78	178.53	63.69	102.2	27.72	179.59	47.35
	2nd Ramp	-	-	-	-	99.73	42.78	177.42	56.8	106.98	27.46	175.55	52.87
	3rd Ramp	-	-	-	-	99.39	48.45	193.1	54.77	104.43	30.72	199.87	56.75

Table 3. Numbers represent spikes per second. Increasing hold duration while maintaining a steady velocity leads to an increase in the slope and number of spikes produced during the hold. In contrast, the maximum and minimum firing rate during the hold increase exponentially as the duration of the hold is decreased.

Vibrations

By applying sinusoidal vibrations to spindle afferents, De-Doncker et al (2003) identified a broader linear range for group II afferents (0.12 – 1 mm) than for Ia afferents (0.12 – 0.25 mm). The linear range indicates the range where the amplitude of the afferent response was directly related to the stretch amplitude. De-Doncker also points out that Ia afferents are more sensitive to high vibration frequencies with small amplitudes than group II afferents. For example, where Ia afferents produce a 1:1 response to 100 Hz vibrations with an amplitude of 0.25 mm, group II afferents are more likely to have the same response to 100 Hz vibrations with an amplitude of 1mm.

Sinusoidal vibrations with amplitudes of 0.08 mm were applied to the gastrocnemius muscle at three different frequencies; 20, 100 and 167 Hz. Responses were collected from 18 control afferents in all. At this amplitude, afferent responses were varied (**Fig 9**). At a vibration frequency of 20 Hz, eleven afferents discharged at 20 Hz during the majority of the sinusoidal cycles. The higher frequencies elicited a similar 1:1 response from a smaller number of afferents; 6/18 at 100 Hz and 3/18 at 167 Hz. Several afferents produced 1:2 and fewer responses while a greater number did not respond at all. Data is not available for afferents lost prematurely before vibrations could be applied due to movement or as a result of the electrode drifting out of the cell.

Of the 18 control afferents that received sinusoidal vibrations, 14 were healthy Ia afferents, 3 were tendon organ afferents and the last was the suspected group II afferent. Twelve of the healthy Ia afferents produced some kind of response to the vibrations. The only similarity found between these afferents is that they all possess initial bursts. There was no correlation between discharge frequency and slope, number of spikes, DI,

maximum IFR, IFR drop, etc. The two afferents that did not respond lacked initial bursts. The suspected group II afferent followed 1:1 with the 20 Hz vibration, but was unable to follow the higher frequency vibrations.

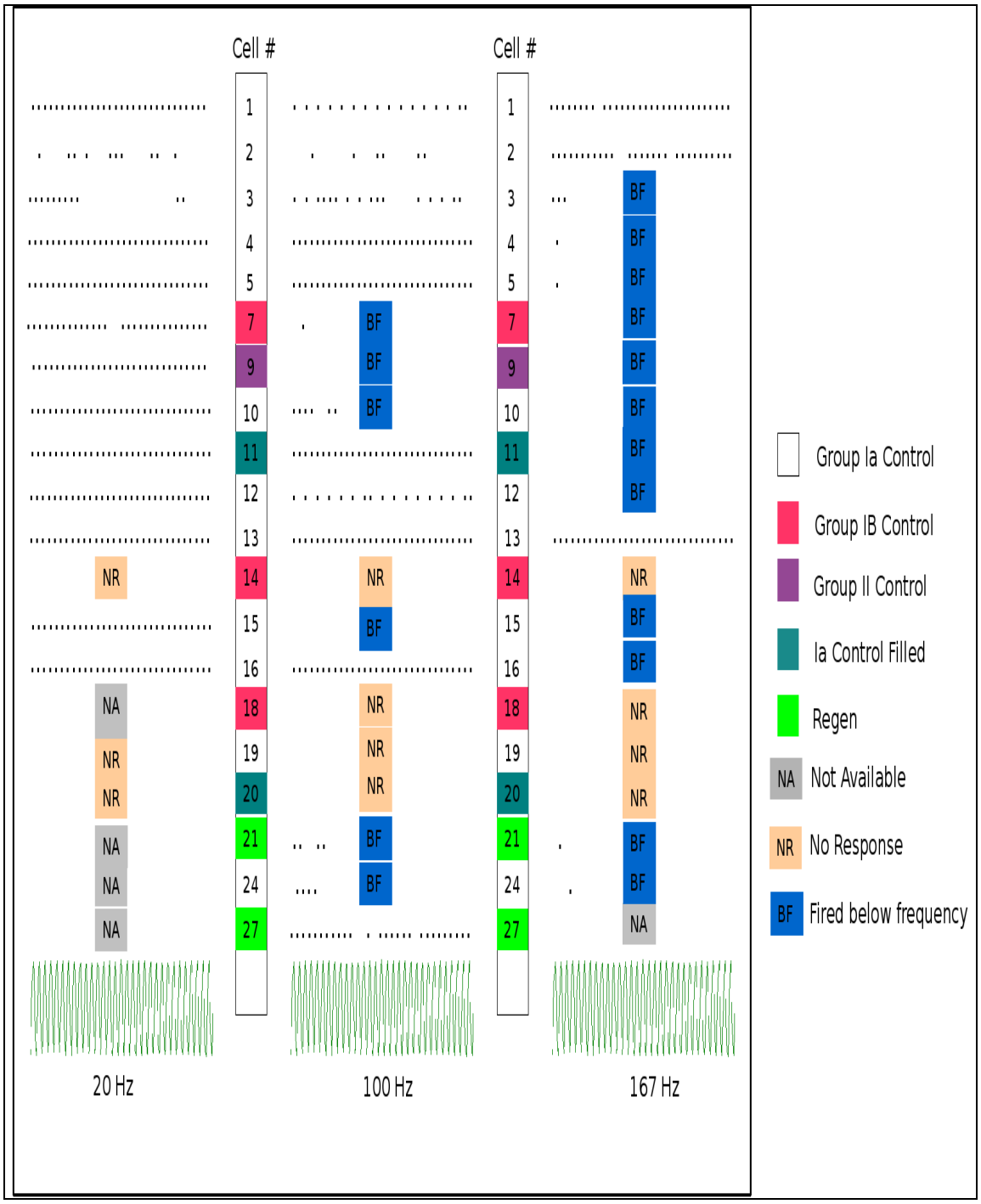

Fig 9. Representation of sinusoidal vibrations applied to afferents. The amplitude for the three frequencies was 1.8 mm. Dots are used to represent afferent firing during a single sine wave. Afferents lacking vibration of a certain frequency are marked NA for not available while afferents that do not discharge at all or discharge are marked NR for no response. BF indicates afferents that discharged at a lower frequency than the applied vibration.

Regenerated Afferents

Each of the regenerated afferent was identifiable as muscle spindle afferents based on their isometric twitch responses. Two of the regenerated afferents regained near-normal encoding abilities, producing initial bursts in response to stretch of the reinnervated gastrocnemius (**Figs 5, 7**). The total number of spikes produced during three triangular stretch ranged between 30 and 80 pps. High IFR drops indicate these two afferents are group Ia afferents. The afferents also had less than 1:1 response to all applied vibration frequencies (**Fig 9**). Normal primary spindle afferent responses suggests the two afferents were primary spindle afferents before nerve transection and recovered their original functions after reinnervation.

The third regenerated afferent appears to be a group II spindle afferent. The DI was as high as 169 pps, much higher than control Ia afferents with IFR drops near 40 pps (**Figs 5, 7, 9**). The afferent's IFR drop was far below 40 pps. Characterization of the afferent remains ambiguous since a possibility exists that the afferent is really a primary or other type of afferent that did not recover properly.

Immunohistochemical Results

Overall VGLUT1 Labeling

The three primary afferents selected for quantitative analysis were clearly labeled by neurobiotin (**Fig 12**). VGLUT1 immunoreactive boutons were randomly selected for analysis. For this exercise, synaptic terminals were not labeled with SV2 to identify synaptic vesicles, therefore, boutons were only identified as protrusions on the afferent with VGLUT1 immunoreactivity.

Using Fluoview software, the fluorescence intensities as well as the cross-sectional areas and Z position of each bouton were calculated. Immunostaining penetration is depicted in **Figure 10**, a plot of VGLUT1 intensity for each of the three neurobiotin-stained afferents with respect to the Z Position. Triton X100 was used to increase penetration of the antibody. Two sets of tissue sections were cut at 50 μm while the third was cut at 100 μm due to tissue softness. The confocal images of the third tissue appear to be less intense near the center of the stack, possibly due to the laser being unable to penetrate the thick cross sections.

VGLUT1 intensities ranged from 570 – 3878 with an average of 2070 ± 756 SD. All 395 boutons studied had average VGLUT1 fluorescence higher than twice the standard deviation (2*SD) of the average background intensity. **Table 4** shows average bouton intensities as well as size for each of the three afferents studied, separated by laminae. The most intense boutons were located in lamina V, while VGLUT1 expression is similar in laminae VII and IX. The majority of boutons in lamina V had fluorescence intensity between 2500 and 3000 with an average of 2598 ± 745 SD. Bouton intensities

were mostly between 1000 – 2000 (average 1818 ± 602 SD) in lamina VII but were more evenly distributed in lamina IX (average 1844 ± 679 SD). VGLUT1 intensity distribution histogram as well as VGLUT1 distribution across total surface area are shown in **Figure 11,** while **Figure 12** shows confocal images for the different laminae.

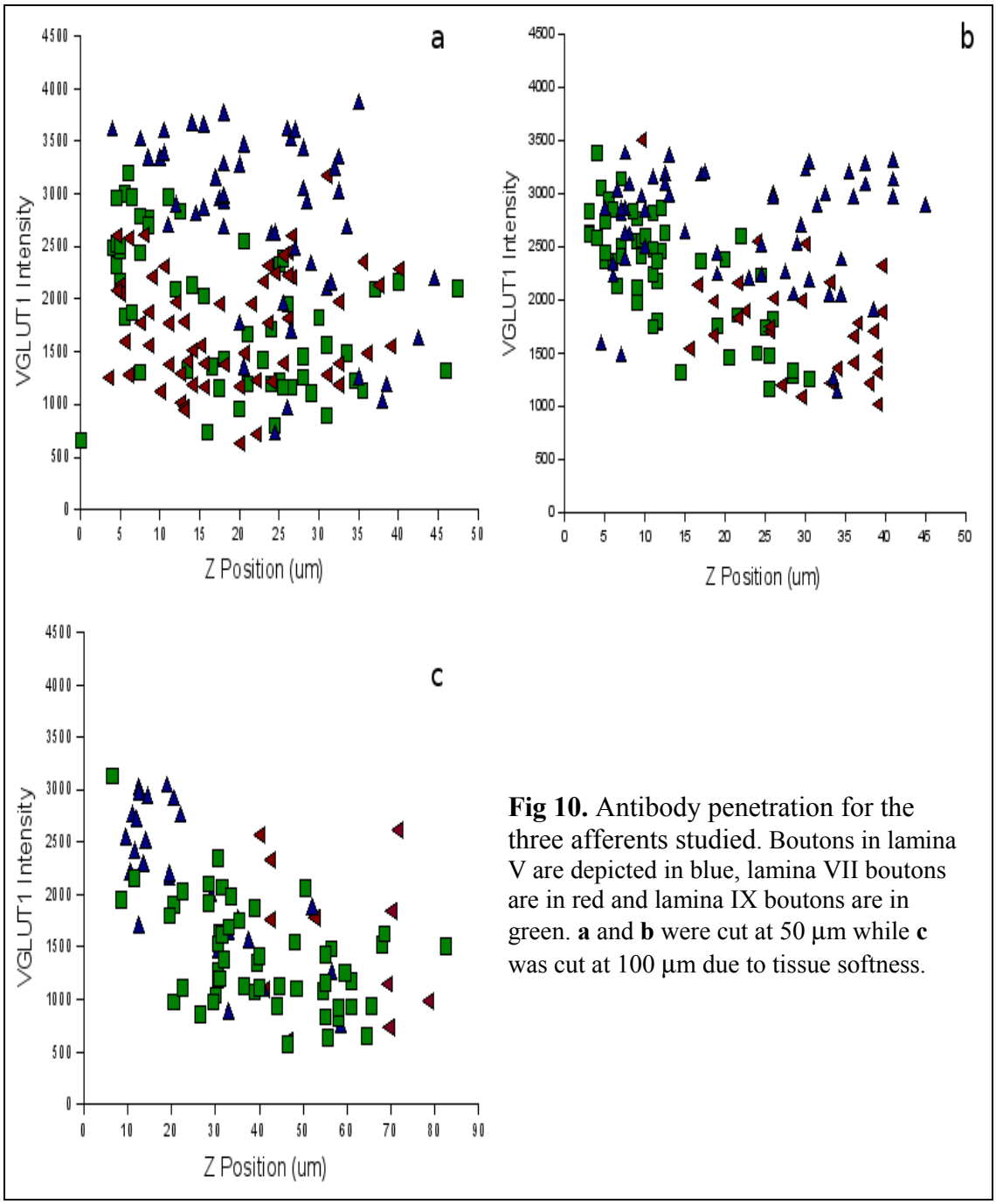

Fig 10. Antibody penetration for the three afferents studied. Boutons in lamina V are depicted in blue, lamina VII boutons are in red and lamina IX boutons are in green. **a** and **b** were cut at 50 µm while **c** was cut at 100 µm due to tissue softness.

In immunocytochemical studies on Ia afferents, Pierce and Mendell (1993) determined that the total number of vesicles as well as vesicles located in the active zone are related to the volume of the bouton. The number of vesicles scale in proportion to the volume of the bouton, making the average percentage of vesicles constant across all bouton volumes. Across the total surface area on the other hand, VGLUT1 distribution is completely random, with r coefficients less than 0.2 across all laminae (**Fig 11**). Bouton sizes are skewed towards smaller values, a phenomenon also observed by Pierce and Mendell (1993).

		Area (um^2)	VGLUT1
Total VGLUT1	Average	5.04	2070.43
	Standard Dev	2.95	765.75
	Max	22.91	3878.88
	Min	0.73	570.64
	n	395	
Lamina V	Average	5.2	2598.95
	Standard Dev	3.24	745.44
	Max	22.91	3878.88
	Min	1.35	735.52
	n	122	
Lamina VII	Average	4.86	1818.67
	Standard Dev	2.78	602.28
	Max	15.51	3500.91
	Min	1.11	611.66
	n	109	
Lamina IX	Average	5.04	1844.6
	Standard Dev	2.83	679.52
	Max	19.46	3375.32
	Min	0.73	570.64
	n	164	

Table 4. VGLUT1 intensities as well as areas for all three afferents with background intensities accounted for. Lamina V boutons appear more fluorescent than the other two laminae.

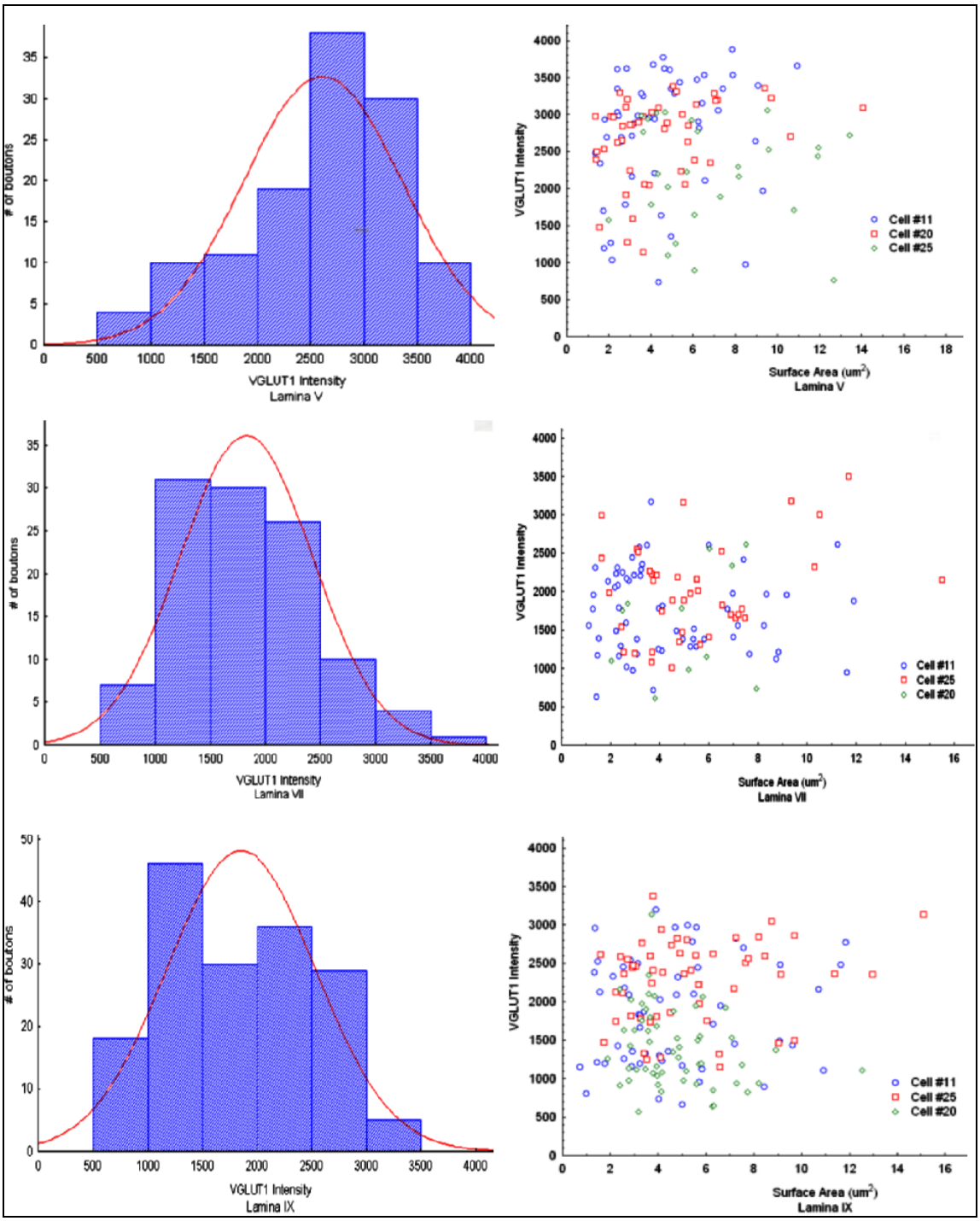

Fig 11. VGLUT1 average intensity distribution for all three afferents. Average VGLUT1 intensity is highest in lamina V but similar in laminae VII and IX. Surface area is skewed towards lower values across all laminae and appears to have no correlation with VGLUT1 intensity.

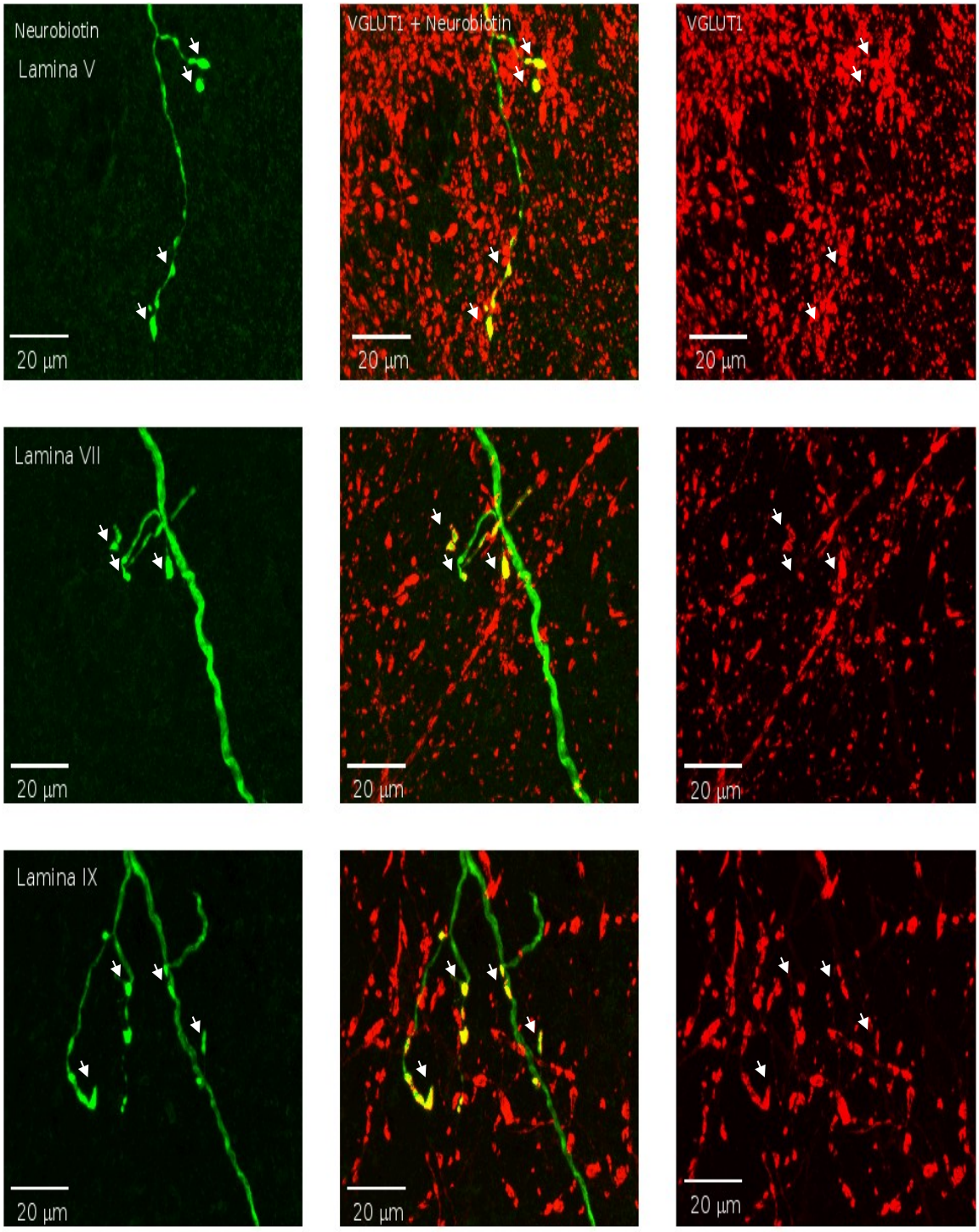

Fig 12. An afferent previously identified as a primary spindle afferent innervating the gastrocnemius muscle was labeled with neurobiotin (green). Cross sections of the spinal cord were stained with VGLUT1 (red). Colocalizations of the two antibodies identify central terminals along the filled afferent. Arrows indicated labeled Ia afferent bouton locations.

Overall VGLUT2 Labeling

Using the same techniques mentioned above, VGLUT2 intensities were measured for randomly selected boutons. Average VGLUT2 fluorescence intensity with background accounted for was 146 ± 118 SD (**Table 5**). The majority of boutons in the first afferent (cell 11) had average VGLUT2 intensities greater than the average background intensity. A total of 96% of the boutons in this afferent possessed more VGLUT2 immunofluorescence than the maximum standard deviation of the average background intensity (1*SD), whereas 80% had more VGLUT2 immunofluorescence than twice the standard deviation of the average background intensity (2*SD). The percentage was lower in the second afferent and third afferents (cell 25 and cell 21), with 61% of boutons in cell 25 having VGLUT2 imunofluorescence less 1*SD and 40% less than 2*SD. Cell 21 had an even lower percentage; 13% of boutons were less than 1*SD and 3% of boutons were less than 2*SD.

Since none of the boutons observed possessed any obvious VGLUT2 immunoreactivity (**Fig 13**), the recorded values are attributed to overlap of the FITC and Cy3 emission spectra. A large amount of crosstalk existed between the two fluorochromes, and may possibly have been eliminated with more stringent filters. Negative VGLUT2 values are a result of background intensities obtained from Z positions with slightly higher intensities than the highest contour slice of the bouton.

The average surface area measured for boutons during this exercise was 6.13 μm^2, a whole μm larger than boutons expressing VGLUT1. Since the tissue all came from the same animals, a reasonable conclusion would be that lacking visual cues such as those afforded by VGLUT1 immunoreactivity, random protrusions other than synaptic

terminals were included in the analysis. Another possibility is that larger terminals lacking VGLUT1 expression were not included in the VGLUT1 analysis. Applying antibodies such as SV2 to illuminate synaptic vesicles in further studies will be useful to avoid such complications.

		Area (um^2)	VGLUT2
Total VGLUT2	Average	6.13	146.78
	Standard Dev	3.58	118.52
	Max	23.03	575.68
	Min	1.2	-118.63
	Count	324	
Lamina V	Average	5.75	138.86
	Standard Dev	3.18	105.46
	Max	21.56	518.16
	Min	1.51	-118.63
	Count	150	
Lamina VII	Average	5.54	161.76
	Standard Dev	1.2	-19.17
	Max	16.07	570.54
	Min	3.11	133.62
	Count	69	
Lamina IX	Average	7.14	148.43
	Standard Dev	1.91	-18.49
	Max	23.03	575.68
	Min	4.23	125.84
	Count	102	

Table 5. VGLUT2 immunoreactivity is non existent on primary spindle afferents. The low values shown here can be attributed to background staining. Negative values are a result of background intensities obtained from Z positions with more intensity than the highest contour slice of the selected bouton.

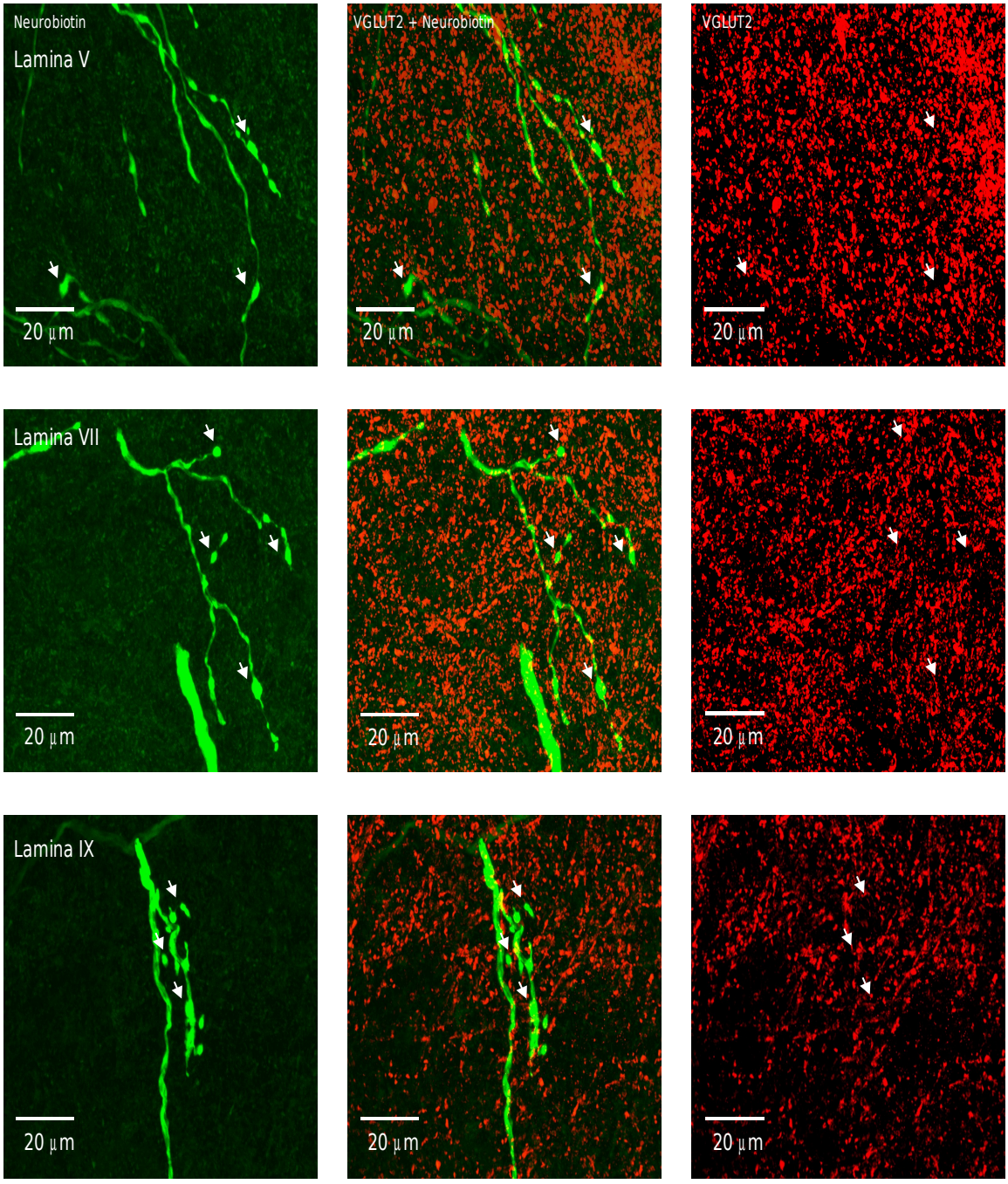

Fig 13. An afferent previously identified as a primary spindle afferent is stained with neurobiotin (green). Cross sections of the spinal cord are stained with VGLUT2 (red). The lack of colocalizations between the two antibodies confirms the absence of VGLUT2 in primary spindle afferents. Arrows indicated labeled Ia afferent bouton locations.

Overall GAD65 Labeling

GAD65 immunoreactive boutons in laminae V, VII and IX were found in clusters surrounding various terminals on each of the three labeled afferents. The number of contacts surrounding randomly selected terminals was counted and the surface area of each contacted bouton measured. Once again, boutons were assumed to be protrusions along the neurobiotin-labeled afferent, especially in regions with few GAD contacts.

The average surface area of the protrusions assumed to be boutons was 5.94 μm^2 (**Table 6**). The majority of GAD65 boutons contacting our labeled afferents were located in lamina IX, with an average of 3.76 contacts per afferent terminal. These results are in agreement with Hughes et al 2005 where the average number of GAD contacts in lamina IX was 3.6 contacts per Ia afferent terminal. A very small number of lamina IX terminals (2-4) lack GAD contacts and they all have boutons with surface areas below 1 μm^2 (**Fig 14**). While GAD65 intense boutons are numerous in laminae V and VII, most of the neurobiotin-labeled boutons in those laminae lack any GAD contacts (**Figs 14, 15**). Neurobiotin labeled boutons located in lamina V have the fewest number of GAD contacts, with an average of 1.25 contacts per bouton, while lamina VII has an average of 2.28 contacts per bouton.

A strong relationship exists between the size of the Ia bouton and the number of surrounding GAD65 intense boutons. This relationship is highly pronounced in lamina IX where the afferent makes contact with the motor neuron pool. Few boutons in lamina V possess GAD65 contacts, therefore this lamina was excluded from comparison. Lamina VII and IX boutons on the other hand, demonstrate distinct relationships between size and GAD65 contacts ($r = 0.61$ for lamina VII and $r = 0.73$ for lamina IX).

		Area (um^2)	GAD Contacts
Total GAD65	Avg	5.94	2.41
	Min	1.28	0
	Max	24.87	14
	Stdev	3.34	2.26
	Count	314	
Lamina V	Avg	6.19	1.25
	Min	1.58	0
	Max	24.87	7
	Stdev	3.65	1.59
	Count	121	
Lamina VII	Avg	5.79	2.28
	Min	1.37	0
	Max	16.97	7
	Stdev	3.19	2.02
	Count	80	
Lamina IX	Avg	5.78	3.76
	Min	1.28	0
	Max	22.83	14
	Stdev	3.11	2.31
	Count	113	

Table 6. Primary spindle afferents experience the least amount of GABA-ergic presynaptic inhibition in lamina V as evidenced by the low number of contacts with GAD65 immunoreactive boutons in that lamina. Ia afferent boutons in lamina IX are subject to the most presynaptic inhibition.

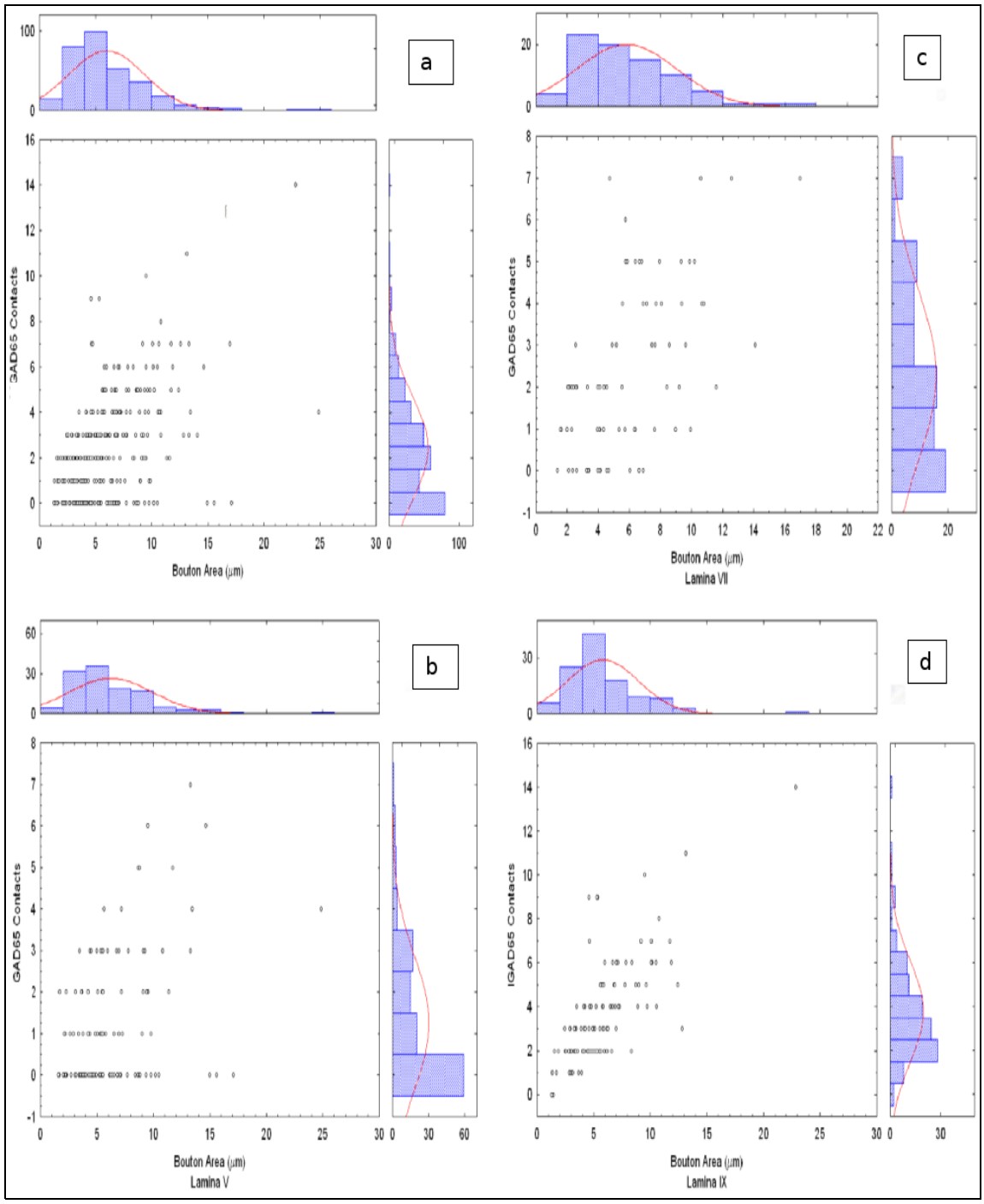

Fig 14. Ia afferent terminals in lamina V receive the least presynaptic inhibition from neurons that express GAD65. The majority of terminals in laminae V and VII receive no presynaptic inhibition, while terminals in lamina IX receive on average 3.76 GAD65 contacts. Less than 4 lamina IX terminals lack presynaptic inhibition and those terminals possess small boutons. Average bouton surface area is directly related to the amount of presynaptic inhibition.

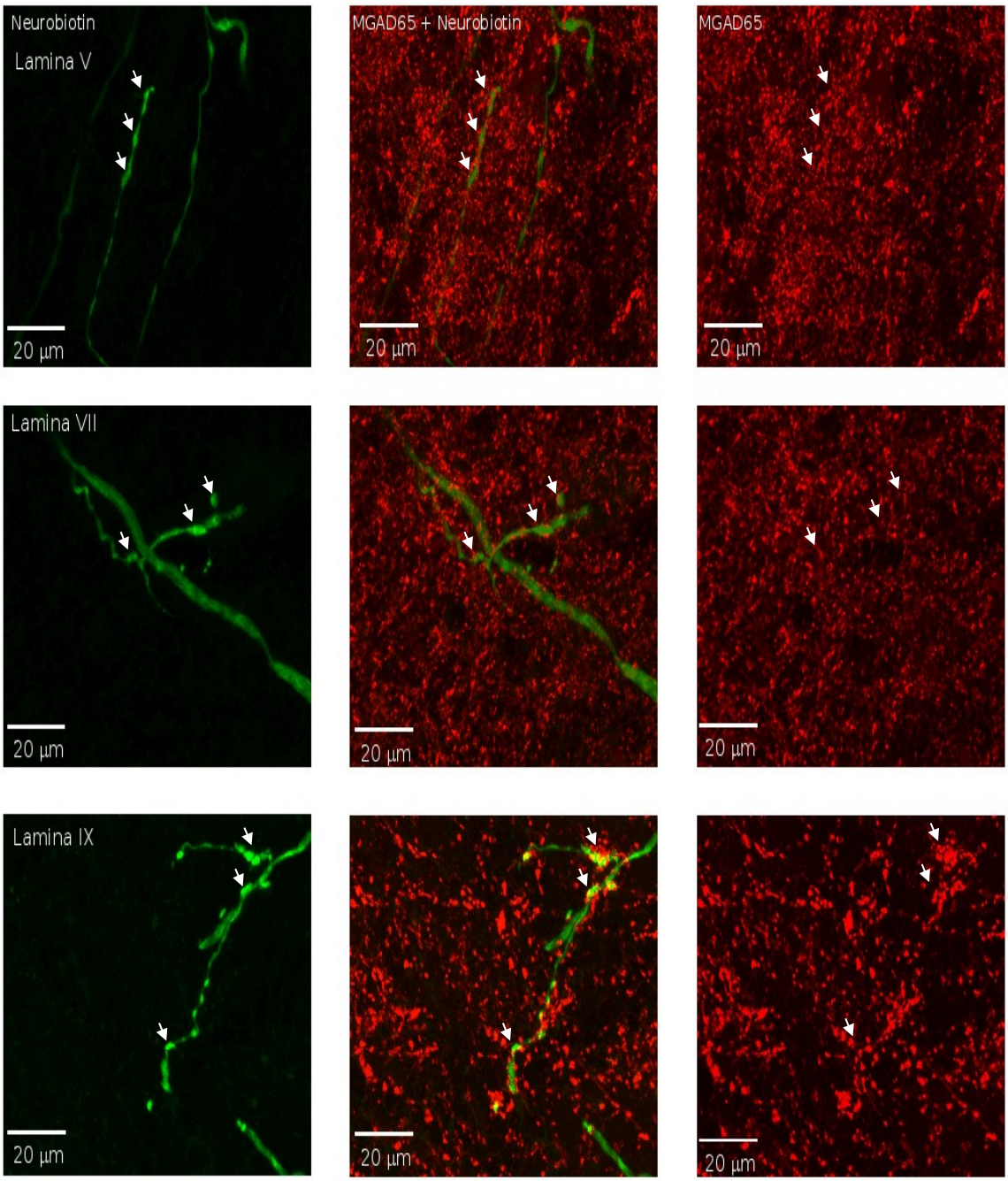

Fig 15. An afferent previously identified as a primary spindle afferent is stained with neurobiotin (green). Cross sections of the spinal cord are stained with the GABA synthesizing enzyme GAD65 (red). GAD65 intense boutons are mostly clustered around central terminals of the filled afferent in lamina IX. Arrows indicated labeled Ia afferent bouton locations.

Labeled afferents: Physiology and Morphology

Three afferents were selected from the group of 24 control afferents and filled with neurobiotin. The afferents' responses to three triangular stretch, ramp and hold stretch as well as vibrations were recorded before they were filled. Each of the three afferents possessed an isometric twitch response indicative of spindle afferents (**Fig 2**).

The three afferents' responses to 3 mm three triangular stretch was also in line with the other spindle afferents (**Table 7a**). Two out of the three afferents produced an initial burst in response to the stretch. All three afferents possessed a moderate IFR max and IFR drops were above 40 pps, an indication that they are indeed Ia afferents. Responses to ramp and hold stretches are also in accord with other spindle afferents studied (**Table 7b**).

Once in the spinal cord, primary afferents bifurcate multiple times, forming numerous contacts in laminae V-VII as well as lamina IX. The neurobiotin dye effectively exposed all three afferents' bifurcations running ventrolaterally from the dorsal horn to the motor neuron pool in lamina IX. The two afferents with initial bursts (cells 11 and 25) had a large number of contacts in those laminae, while the majority of the third afferent's (cell 20) bifurcations were located in lamina IX.

The total number of contacts recorded for cell 20 in laminae V and VII are approximately 50 each. In lamina V, 27 and 17 boutons were stained with VGLUT1 and GAD65 respectively. Lamina VII had a few more contacts, with 11 and 49 boutons stained respectively with VGLUT1 and GAD65. For one of the other afferents (cell 11), GAD65 contacts in laminae VII and IX could not be visualized due to prolonged exposure of the tissue. The dye tracer was bleached out as a result and reapplying

streptavidin-FITC had no effect on re-exposing the filled afferent.

VGLUT1 intensity in laminae V and VII was generally similar for cells 11 and 25 with lamina V boutons predominantly in the range of 2500 – 3500 and lamina VII boutons mostly between 1000 and 2500. The third afferent matches the other two in lamina V, but the low number of VGLUT1 boutons in lamina VII (n = 11) precludes any conclusions about that lamina. VGLUT1 intensity in lamina IX is similarly distributed for cells 11 and 20, with a majority of boutons concentrated in the 1000 – 2000 range. Cell 25, on the other hand, has more VGLUT1 intense boutons (average 2680) in lamina IX (**Fig 16**).

GAD65 contacts in lamina V were similar for cells 11 and 25, with a majority of boutons lacking presynaptic inhibition. The number of lamina V boutons for cell 20 (n = 17) is too low to form an unambiguous conclusion. In laminae VII and IX, cell 20 has an average number of 2.96 contacts per bouton while cell 25 has an average of 1.19 contacts. Unlike cell 20, the majority of lamina VII boutons for cell 25 once again lack presynaptic inhibition. The number of GAD65 contacts increases for both afferents in lamina IX, with an average of 3.76 contacts per bouton. All lamina IX boutons in cell 25 have at least one contact, while cell 20 has a couple of small sized boutons without presynaptic inhibition (**Fig 16**).

With the least amount of GAD contacts and the highest VGLUT1 intensity in lamina V, cell 11 has a low initial burst as well as the lowest overall physiological response. The other afferent with a higher initial burst (cell 25) had more GAD contacts and lower VGLUT1 intensity in lamina V. Lacking an initial burst in the third afferent, we are unable to draw a suitable conclusion. More data is needed to determine whether whether these three factors are related.

Many similarities exist physiologically between cells 20 and 25 (DI, IFR drop, IFR max). However, these similarities do not necessarily translate to morphological compatibilities. Cell 20 has more GAD contacts and less VGLUT1 intensity than cell 25. The ratio of VGLUT1 intensity between lamina V and the other two laminae is similar in the two afferents, but the ratio of GAD65 contacts for those laminae differs in the afferents.

a

		Cell #11	Cell #25	Cell #20
IB	1st Triangle	77.88	141.84	-
Slope	1st Triangle	16.26	18.41	28.62
	2nd Triangle	28.52	31.71	41.49
	3rd Triangle	28.83	32.11	43.47
Spikes	1st Triangle	50	66	53
	2nd Triangle	31	46	33
	3rd Triangle	28	43	32
IFR Drop	1st Triangle	85.8	117.16	88.21
	2nd Triangle	82.78	116.54	66.99
	3rd Triangle	82.78	104.72	103.6
IFR Max	1st Triangle	86.81	120.48	107.53
	2nd Triangle	83.75	117.65	106.95
	3rd Triangle	81.3	114.29	103.63

Table 7. Numbers represent spikes per second. The three filled afferents can be characterized as spindle afferents based on their initial bursts, number of spikes, slope and history dependence. High maximum IFRs and moderate DI further identify them as Ia afferents. Responses to three triangular (**a**) and ramp and hold stretch (**b**) are similar to other control spindle afferents studied.

b

		Cell #11	Cell #25	Cell #20
Ramp Total (s) / Hold (s)		0.5 / 0.2	1.3 / 1	1.3 / 1
IB	1st Ramp	273.22	416.67	-
	2nd Ramp	268.82	400	-
	3rd Ramp	264.55	392.16	-
Slope Rise	1st Ramp	28.22	22.34	61.03
	2nd Ramp	28.39	26.8	77.37
	3rd Ramp	24.1	26.58	75.25
Slope Hold	1st Ramp	-46.01	-35.25	-20.52
	2nd Ramp	-54.62	-35.72	-20.87
	3rd Ramp	-51.25	-36.76	-21.19
Spikes Rise	1st Ramp	15	22	14
	2nd Ramp	15	22	12
	3rd Ramp	15	21	11
Spikes Hold	1st Ramp	12	68	54
	2nd Ramp	12	68	50
	3rd Ramp	12	67	49
Hold Max	1st Ramp	66.14	95.24	70.42
	2nd Ramp	69.74	94.34	66.23
	3rd Ramp	68.59	98.04	64.1
Hold Min	1st Ramp	57.67	52.08	46.3
	2nd Ramp	54.82	46.84	43.01
	3rd Ramp	55.74	46.4	40.08
IFR Drop	1st Ramp	69.87	100.88	108.01
	2nd Ramp	78.78	91.77	109.42
	3rd Ramp	71.9	101.71	107.84
IFR Max	1st Ramp	126.26	162.6	169.49
	2nd Ramp	127.23	172.41	172.41
	3rd Ramp	121.65	173.91	169.49
DI	1st Ramp	-	93.4	116.72
	2nd Ramp	-	104.62	124.68
	3rd Ramp	-	111.02	123.83

		Lamina V		Lamina VII		Lamina IX	
		VGLUT1 Intensity	MGAD65 Contacts	VGLUT1 Intensity	MGAD65 Contacts	VGLUT1 Intensity	MGAD65 Contacts
Cell 11	Average	2753.94	0.74	1739.14		1862.9	
	StDev	834.17	1.17	545.71		687.29	
		n = 50	*n = 50*	*n = 59*		*n = 57*	
Cell 25	Average	2680.64	1.26	2004.08	1.19	2274.24	3.6
	StDev	567.81	1.47	616.25	1.3	537.56	1.89
		n = 45	*n = 54*	*n = 39*	*n = 31*	*n = 53*	*n = 62*
Cell 20	Average	2175.79	2.71	1587.83	2.96	1403.59	3.96
	StDev	696.66	2.14	719.2	2.1	504.34	2.73
		n = 27	*n = 17*	*n = 11*	*n = 49*	*n = 54*	*n = 51*

Table 8. VGLUT1 intensity appears to be inversely related to the number of GAD65 contacts in lamina V. While GAD contacts are similar in laminae V and VII, VGLUT1 intensity in lamina VII is similar to lamina IX which has the highest presynaptic inhibition. GAD65 contacts in laminae VII and IX were unavailable for cell 11.

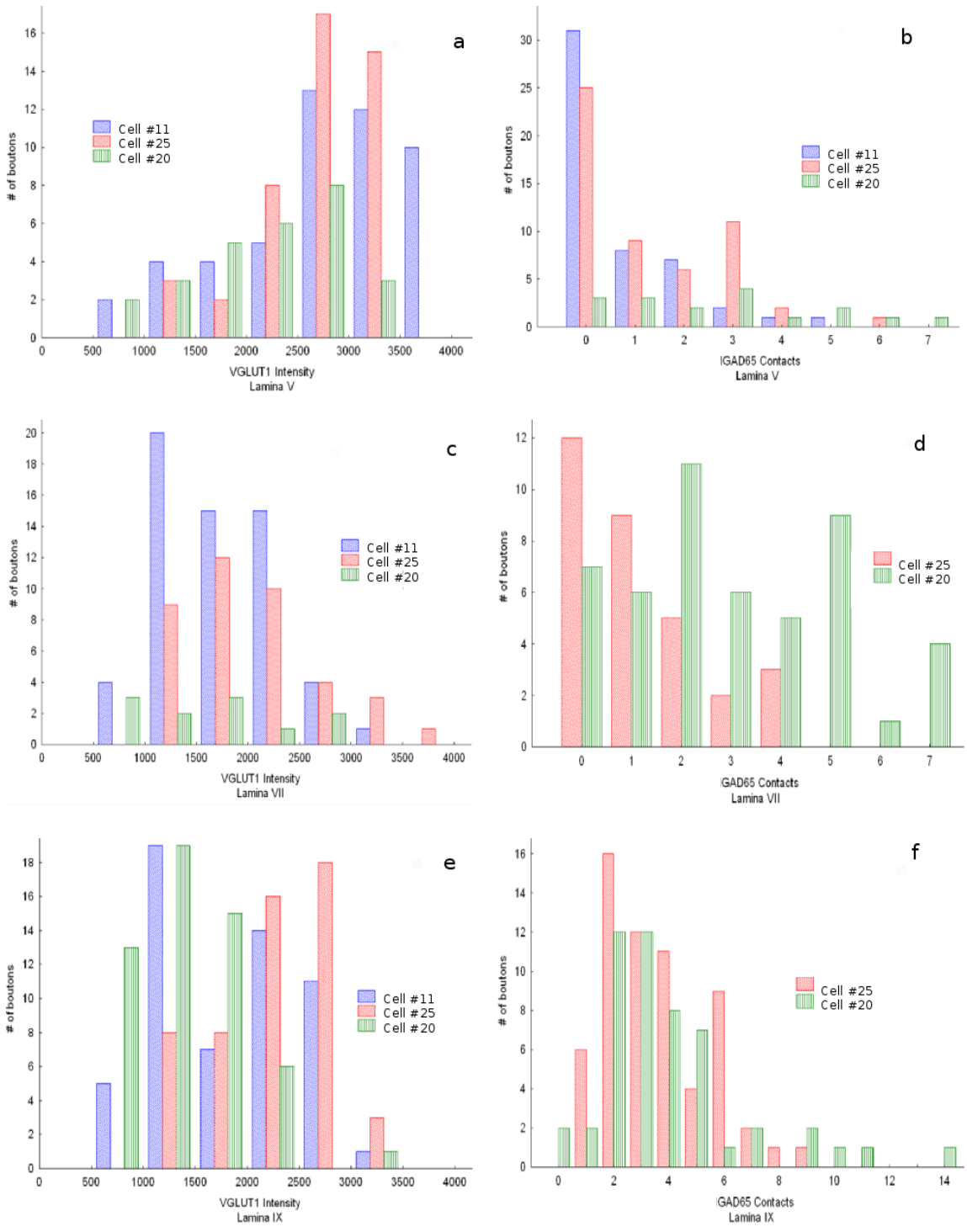

Fig 16. VGLUT1 intensity and number of GAD65 contacts for each afferent separated by laminae. GAD65 data is unavailable in laminae VII and IX for cell #11.

Discussion

Peripheral injury causes many physiological and morphological changes in the primary afferent – motor neuron circuit, changes which are not all reversed after afferent regeneration and reinnervation of the muscle (Gregory et al 1982, Lewin and McMahon 1991). Successful reinnervation occurs in only about 75% of muscle spindles and many sensory fibers end up innervating muscles other than those they originally supplied (Collins et al 1986, Burges and Horch 1973, Lewin and McMahon 1991a,b). While the circuit recovers the ability to transmit action potentials and generate EPSPs in response to electrical stimulation, stretch evoked EPSPs are non existent after regeneration (Haftel et al 2005).

We embarked upon this study to evaluate the effects of regeneration on synaptic transmission. The final post-regeneration results have yet to be obtained; therefore this thesis presents preliminary data that will be used to assess the results of studies conducted on regenerated afferents. By documenting synaptic protein expression in healthy animals, we are able to develop a standard to measure the amount of presynaptic inhibition as well as excitatory synaptic transmissions in regenerated primary spindle afferents.

In the present study, primary spindle afferents were identified by their responses to a variety of electrophysiological stimuli. Criteria used for characterization included isometric twitch response, the presence of initial bursts, history dependence, IFR drop, maximum IFR and finally dynamic index. This approach allowed for easy identification of all the afferents studied, including group Ia, II and tendon organ afferents. Three of the characterized Ia afferents were selected for immunohistochemical analysis after filling with neurobiotin.

Novel Findings

The vesicular glutamate transporters (VGLUTs) 1 and 2 are known to be differentially distributed within the spinal cord. While VGLUT2 is expressed throughout the spinal cord gray matter, VGLUT1 is the only isotype present at the central terminals of primary spindle afferents. During the course of this study, we observed a variation in VGLUT1 distribution within the various Rexed laminae that contain Ia afferent terminations. The most abundant VGLUT1 distribution was in lamina V, where Ia afferents form excitatory synapses with a large group of small interneurons involved in the non-reciprocal inhibitory circuit (Jankowska et al, 1981). The average VGLUT1 intensity in lamina V was over 30% higher than in the other two laminae studied (**Table 8**). Despite having vastly different postsynaptic elements, laminae VII and IX contained very similar VGLUT1 distributions.

In comparing the laminae distribution of GAD65-intense boutons that provide presynaptic inhibitory input to Ia afferent terminals, lamina V appeared to be the region with the least number of inhibitory contacts. Lamina VII had a slightly higher number of GAD65 contacts per bouton, but the greatest amount of presynaptic inhibitory input was in lamina X. These results raise the question whether VGLUT1 expression is inversely related to the amount of presynaptic inhibition. Alternatively, low presynaptic inhibition may be conducive to higher VGLUT1 expression as observed in lamina V, whereas the opposite applies in lamina IX. Further investigation into the matter is required.

While a relationship between VGLUT1 expression and the level of presynaptic inhibition remains unclear, we did find that a linear relationship exists between bouton surface area and the amount of presynaptic inhibition the bouton experiences (**Fig 14**). Larger surface area provides room for more contacts, therefore, it is no surprise that more

GABA-ergic boutons are found clustered around large Ia boutons, in complete agreement with the synaptic size principle. It may be that the amount of presynaptic inhibition is determined by the probability of transmitter release at that bouton, with large boutons, which may have a higher release probability, subject to more presynaptic inhibition than smaller boutons. While this behavior has yet to be confirmed in Ia afferent collaterals, such a relationship has been observed in crab neuromuscular junctions where synapses that produced large EPSPs had more inhibitory contacts (Tse et al, 1991).

Quantal theory describes the relationship between the probability of release, the postsynaptic response and the number of vesicles using the equation $m = pn$ (Koenig et al, 1989). In the equation, m represents the mean quantal content, which effectively translates into the amplitude of the postsynaptic response. The probability of release is represented by p, and n is the number of vesicles. According to this equation, release probability increases if quantal content goes up while the number of vesicles remain the same ($p = m/n$). Release probability also increases when the number of vesicles is reduced if a constant quantal content is maintained. With larger Ia afferent boutons, the number of vesicles is likely greater, but a larger quantal content can offset the number of vesicles, increasing the probability of transmitter release at the synapse.

A lower probability of release could also explain the amount of GAD65-intense contacts at Ia afferent terminals located in laminae V, VII and IX. With a greater number of synaptic vesicles, as indicated by the higher VGLUT1 expression, lamina V boutons would have a lower release probability if the quantal content was the same as lamina IX. If lamina VII boutons had low quantal content in addition to a lesser number of vesicles, the release probability at those terminals would remain low. Lamina IX boutons, on the other hand, could have a higher release probability due to having a positive combination

of quantal content and vesicle count.

Physiology and relation to synaptic protein expression

Physiology and synaptic morphology are intricately linked, with changes in one often mirrored in the other. For example, longer neuromuscular junction active zones are found at synapses with high output and prolonged stimulation of the synapse results in changes in physiological as well as morphological properties (Govind and Chiang, 1979; Propst and Ko, 1987; Atwood and Marin, 1983). Similarly, stimulating tonic and phasic motor axons in lobster and crayfish respectively, results in increases in mitochondrial size and number, vesicle accumulation and transmitter release (Lnenicka et al, 1986; Chiang and Govind, 1986).

In comparing physiology to morphological properties, a number of variabilities are evident in the three selected afferents. The small sample size used in this study raises obstacles against identifying trends. We did not observe any obvious correlations between instantaneous firing rate during any of the stretches applied and either VGLUT1 expression or GAD65 contacts. However, the afferent with the highest initial burst frequency also possessed a moderately large number of GAD65 contacts. It may be that there exists a relationship between the frequency of the initial burst and the number of surrounding GAD65 contacts (**Tables 7, 8)**. Were this the case, such a relationship would be in agreement with findings by Prochazka and collaborators (1976) suggesting that low vesicle count may promote a higher physiological response. This speculation was raised by the observation that afferents capable of firing at frequencies up to 500 Hz tend to have boutons with a low number of vesicles (Prochazka et al, 1976). The high number of

GAD65 contacts observed in our study could promote fewer vesicles and subsequently, a higher physiological response. A more intensive study is required to confirm whether such a relationship exists.

Synaptic protein expression variations in different laminae

VGLUT1 intensity in central terminals of Ia afferents appears highest in lamina V, the region where the afferents form excitatory contact various non-reciprocal interneurons. Central terminals belonging to Ia afferents in this region were densely packed and possessed the least number of GAD65 contacts compared to the other laminae. In lamina V, Ia afferents excite inhibitory neurons with descending collaterals to homonymous and synergistic motor neurons (Jankowska et al, 1981; Brink et al, 1983; Hongo et al, 1983). These interneurons are co-excited by primary muscle spindle and tendon organ afferents and are therefore known as non-reciprocal inhibitory interneurons (Jankowska et al, 1981; Hughes et al, 2005). The amount of GAD65-intense P boutons in contact with Ia afferent boutons in lamina IX is likely a result of the high VGLUT1 content and numerous Ia afferent collaterals in lamina V. The functional significance of the low number of GAD65 contacts in lamina V is not yet clear, although it should be noted that Ia and tendon organ afferents inhibit each other in that lamina (Jankowska et al, 1981).

Ia afferent collaterals in laminae VII and IX contain approximately the same amount of VGLUT1 immunoreactivity, yet inhibitory input to Ia afferents in lamina IX far exceeds that in lamina VII. Ia afferents receive more inhibitory input in lamina VII than V, therefore, the source of inhibition in lamina VII may explain the level of

inhibition in the lamina. Antagonistic interneurons, termed Ia reciprocal inhibitory interneurons, mediate inhibition in lamina VII (Jankowska et al, 1972a, b). Our results, therefore, suggest that homonymous and synergistic afferents play a larger role in Ia afferent inhibition than do antagonists.

The variation in VGLUT1 expression within Ia afferent central terminals located in laminae V and IX may be significant when considering the amount of VGLUT1 depletion observed in the two laminae after peripheral injury. Depletion of the protein is gradual and is most pronounced in lamina IX where over 80% is lost by the end of the 4th week (Hughes, 2004). Lamina V boutons, on the other hand, lose between 50 – 70% of their VGLUT1 immunoreactivity during the same period. It may be that the same amounts of VGLUT1 molecules are lost in both laminae. However, laminae IX would appear more depleted since it had a smaller number of transporters to start with.

Bouton surface area as a measure of protein expression

The synaptic size principle of Pierce and Mendell (1993) postulates that bouton volume is strongly related to the total number of vesicles found at Ia terminals. Not only does the number of vesicles increase as boutons grow larger, so do the active zones and the number of vesicles bound by synapsin I cross linkages at these active zones (Pierce and Mendell 1993). Vesicles located at active zones are associated with a readily available pool, whose size is linked to synaptic output. The size of active zone vesicles, and therefore the probability of release, is modulated by activity levels.

While total volume determines vesicle number and subsequent VGLUT1 expression, our data suggests that surface area has no bearing on these values (**Fig 10**).

Apposed surface area has been shown to have a strong correlation to bouton volume and conversely with vesicle number (Nam et al 2002, Pierce and Mendell 1993). These results are intriguing because one would expect to see a larger number of vesicles in boutons with more surface area. However, our study measured the average VGLUT1 distribution in each bouton, which may be the determining factor in the random distribution we observed.

Another explanation for the deviation from expected result is the difference between surface area and volume. By definition, a small variation in bouton length or width can increase the volume exponentially while barely affecting the surface area. With increased volume comes larger active zones and more vesicles clustered around said active zones. Despite a larger number of total vesicles, more surface area may go unused due to the dense concentration of vesicles around the available active zones. The lack of a relationship that we observed between surface area and average VGLUT1 intensity we observed may be attributed to this.

Regeneration has been shown to have an adverse effect on bouton size (Koerber et al, 1994). Quantitative analysis of regenerated cutaneous afferents by Koerber et al (1994) showed a marked reduction in the size of boutons from the regenerated afferents compared to controls. Terminal arborizations from regenerated afferents were also more likely to be shorter than healthy afferents. If the relationship between bouton size and presynaptic inhibition holds true after regeneration, boutons from regenerated afferents can be expected to have less presynaptic inhibition, possibly as a result of lower overall release probability. Koerber et al's findings (1994) that the regenerated afferents' boutons possessed equal or greater excitability than controls implies that the newly formed terminals either developed more active zones than normal or the terminals lost some

inhibitory input, resulting in less controlled responses than their healthy counterparts. Further study will be required to identify the cause.

The depletion of VGLUT1 at the central terminals of primary afferents observed after peripheral nerve injury may be caused by a number of different factors. The loss of synaptic vesicles, withdrawal of presynaptic boutons, as well as an increase in spontaneous activity in muscle afferents could all contribute to a decrease in the number of VGLUT1 molecules (Alvarez et al, 2000; Castro-Lopez et al, 1990; Chen 1978; Johnson et al, 1991). The smaller bouton size observed by Koerber et al (1994) may be yet another factor that causes VGLUT1 depletion. The smaller surface area may be unable to sustain the number of presynaptic contacts present before the injury, leading to lower levels of VGLUT1. Without knowing whether the abundance of presynaptic inhibitory input precludes VGLUT1 expression, the opposite may also be true. The smaller boutons may simply have fewer synaptic vesicles and subsequently lower VGLUT1 expression. In this case, the bouton could have a decreased level of presynaptic inhibition due to a lower probability of release. Whatever the situation, it is most likely that several factors act together to trigger VGLUT1 depletion in primary afferent central terminals after peripheral nerve injury.

Similarities along arborizations

Many similarities are known to exist between boutons attached to the same terminal arborization. Factors such as volume, number of active zones, number of P boutons and number of vesicles tend to either decrease or stay the same as one moves towards the terminal bouton (Pierce and Mendell, 1993). The terminal boutons often had

the most extreme values in the group, being the boutons with either the largest or the smallest volume, active zones, vesicles and surrounding P boutons.

We made a similar observation in this study, where boutons attached to the same arborizations possessed similar levels of VGLUT1 immunoreactivity and GAD65 contacts. This behavior was especially noticeable in laminae V and VII where few GAD65 contacts exist. The few Ia boutons in these two laminae surrounded by GAD-intense boutons were located on terminal arborizations containing other boutons surrounded by a similar number of contacts. VGLUT1 immunoreactive boutons were also generally surrounded by boutons with similar levels of immunoreactivity. A scattering of boutons broke this pattern, expressing properties in contrast to neighboring boutons. Despite these deviants, a clear pattern of protein expression was visible along arbors.

These observations suggest that boutons attached to the same terminal arborizations make contact with the same or similar neurons and therefore receive similar input. Presynaptic inhibition as well as synaptic depression could affect the majority of boutons along the same terminal branch. In lamina IX specifically, primary afferents synapsing with a particular motor neuron may have the same amount of presynaptic inhibition or depression of transmission. In fact, such complementary presynaptic inhibition at motor neurons has been observed by Clements et al (1987) when measuring the amplitude of EPSPs evoked from several afferents. The study noted such behavior at some Ia afferent – motor neuron synapses, but not all. The exceptions may involve the aberrant boutons mentioned earlier.

Other Considerations

Synaptic plasticity is known to be affected by neural activity or lack thereof,

during development, following nerve trauma or disease and also during learning (Nielsen et al, 1993; Perez and Nielsen, 2004). A downregulation of several proteins and mRNA implicated in spinal plasticity has been observed within 24 hrs following spinal cord injury. The proteins and mRNA proceeded to recover fully after 7-14 days, during the period that coincides with recovery of motor function (Di Giovanni et al, 2005). Other proteins that promote synaptic plasticity are also upregulated after motor function is recovered (Di Giovanni et al, 2004).

These observations raise the question of whether the same activity occurs after peripheral nerve injury. Since VGLUT1 and 2 are thought to be expressed at synapses with high and low plasticity respectively, the short period of low plasticity before recovery of motor function during regeneration may be conducive to an upregulation of VGLUT2 at the central terminals of Ia afferents with low levels of VGLUT1 (Hesler et al, 1993; Rosenmund et al, 1993; Dittman et al, 1998; Fremeau et al, 2004). Several studies have shown that peripheral nerve injury induces functional and structural changes in both monosynaptic and polysynaptic reflex circuits, causing hyperexcitability that appears to be permanent (Koerber et al, 1994; Hellgren and Kellerth, 1989; Valero-Cabre and Navarro, 2001; Navarrete et al, 1990; Vejsada et al, 1991). With VGLUT1 depletion seemingly permanent, VGLUT2 may become the de facto glutamate transporter, perhaps colocalized at terminals expressing low levels of VGLUT1. It is quite possible that the lower level of VGLUT1 expression is sufficient to maintain synaptic transmission after regeneration. Only further studies of regenerated afferents will tell whether the loss of VGLUT1 is followed by an increase in a second glutamate transporter.

One possible explanation for the loss of the monosynaptic stretch reflex after regeneration is that due to the low levels of VGLUT1 in lamina IX Ia afferent terminals,

EPSPs of noteworthy amplitudes cannot be generated by stretch. Were this the case, small stretch evoked EPSPs would be present at motor neuron terminals, perhaps with amplitudes only ~15% of the EPSP amplitudes in healthy animals. No stretch evoked EPSPs are observed however (Haftel et al, 2005). The low level of VGLUT1 coupled with the small amount of cell death that occurs after peripheral axotomy may be responsible for the lack of stretch evoked EPSPs. However, the suspected upregulation of VGLUT2 should provide enough glutamate at motor neuron synapses in response to stimulation.

The apparent recovery of the H-reflex, the electrical counterpart of the monosynaptic stretch reflex, intimates another process may be at work (Valero-Cabré and Navarro, 2001, 2002a). The number of presynaptic inhibitory contacts may increase after regeneration, effectively suppressing transmission at Ia central terminals. Such an increase in inhibition has been observed following spinal cord injury and recovery as well as after partial nerve injury (Tillakaratne et al, 2002; Moore et al, 2002). It would be interesting to know whether presynaptic inhibition in laminae V and VII remain negligible after regeneration.

Technical Limitations

A number of limitations were encountered that rendered impossible complete standardization of tissue processing. First, the distance between the location of the microelectrode and the entry point of the afferent into the spinal cord varied between all afferents. Neurobiotin injection was performed as close to the entry point as possible to decrease the amount of transport time and the distance to the entry point ranged from 3 to

5 mm. The dye was given at least six hours to travel retrogradely through the afferent before perfusion to mitigate the impact of the difference in injection locations.

The quality of the perfusion also varied despite all attempts at standardization. One of the animals expired 5 hours after the neurobiotin injection, leaving the subsequent perfusion ineffective at completely fixing the spinal cord. The cord was very fragile despite an extended post fixation period and cross sections had to be cut at twice the normal thickness, thereby limiting antibody penetration. Background levels were normalized individually for each bouton, taking into account the location of the bouton within the confocal stack in order to minimize the effect of low antibody penetration.

Following tissue processing, cross sections were viewed under a confocal microscope and boutons at central afferent terminals were randomly selected. In most cases, the majority of the available boutons were not analyzed. This raises the possibility that the subpopulation analyzed do not represent all available boutons. This is an issue with any study utilizing a randomly selected subpopulation to represent the whole group. The estimated error rate for this particular part of the study is small.

A final limitation for the study lies in the method used for bouton identification. As dual labeling with SV2 was not used to illuminate synaptic vesicles, boutons were generally assumed to be protrusions visible along the length of the stained afferent. For sections stained with VGLUT1, only protrusions expressing the protein were analyzed. For sections stained with GAD65, synaptic vesicle clusters contacting protrusions along the stained afferent were used to identify some central terminals. Terminals lacking these clusters resided mainly in laminae V and VII and were identifiable only as protrusions. It is quite possible that a few random bumps along the afferents were included and labeled enpassant boutons.

A negligible amount of error can also be attributed to manual tracing of boutons. The software used for analysis, Fluoview FV500, performed calculations on the entirety of the selected area. The viewing area was highly magnified during tracing and care was taken to trace over the edges of the neurobiotin staining. The error introduced during tracing is therefore deemed minute.

Concluding Remarks

The stretch reflex is lost after peripheral nerve transection and regeneration. This occurs despite recovery of the H-reflex, the electrical counterpart of the stretch reflex. Data obtained from this study will be instrumental in identifying whether CNS-mediated modifications at the central terminals of primary spindle afferents are responsible for loss of the stretch reflex. The synaptic proteins measured in this study are the vesicular glutamate transporters (VGLUT) 1 and 2 as well as the GABA synthesizing enzyme GAD65. VGLUT1 expression in Ia central terminals appears highest in lamina V, implying a high level of Ia afferent-mediated motor neuron inhibition. Presynaptic inhibition, in the form of GAD65-intense boutons in contact with Ia afferents, also appears to have a tentative relationship to VGLUT1 expression, as boutons with high VGLUT1 content are generally in contact with fewer GAD65-intense boutons and vice versa. Regeneration after peripheral nerve transection may change the expression patterns and trends observed in healthy animals.

References

Alvarez FJ, Fyffe REW, Dewey DE, Haftel VK and Cope TC (2000) Factors regulating AMPA-type glutamate receptor subunit changes induced by sciatic nerve injury in rats. J Comp Neurol 426: 229 – 242.

Atwood HL and Marin L (1983) Ultrastructure of synapses with different transmitter-releasing characteristics on motor axon terminals of a crab. Hyas areneas. Cell Tissue Res 23 (1): 103 - l15.

Bai L, Xu H, Collins JF and Ghishan FK (2001) Molecular and functional analysis of a novel neuronal vesicular glutamate transporter. J Biol Chem 276: 36764 – 36769.

Bailey CH and Chen M (1989) Time course of structural changes at identified sensory neuron synapses during long-term sensitization in Aplysia. J Neurosci 9: 1774 - 1780.

Barron DH and Matthews BHC (1938) The interpretation of potential changes in the spinal cord. J Physiol Lond 92: 276 - 321.

Bellocchio EE, Hu H, Pohorille A, Chan J, Pickel VM and Edwards RH (1998) The localization of the brain-specific inorganic phosphate transporter suggests a specific presynaptic role in glutamatergic transmission. J Neurosci 18: 8648 – 8659.

Beirowski B, Adalbert R, Wagner D and Coleman M (2005) The progressive nature of Wallerian degeneration in wild-type and slow Wallerian degeneration (Wld^S) nerves. BMC Neurosci 6: 6.

Bellocchio EE, Reimer RJ, Fremeau RT Jr and Edwards RH (2000) Uptake of glutamate into synaptic vesicles by an inorganic phosphate transporter. Science 289: 957 – 960.

Brink E, Harrison PJ, Jankowska E, McCrea DA and Skoog B (1983) Post-synaptic potentials in a population of motoneurones following activity of single interneurones in the cat. J Physiol 343: 341 - 359.

Brown AG and Fyffe REW (1978) The morphology of group ia afferent fibre collaterals in the spinal cord of the cat. J Physiol 274: 111 - 127.

Burgess PR and Horch KW (1973) Specific regeneration of cutaneous fibers in the cat. J Neurophys 36: 101 - l 14.

Castro-Lopes JM, Coimbra A, Grant G and Arvidsson J (1990) Ultrastructural changes of the central scalloped (C1) primary afferent endings of synaptic glomeruli in the substantia gelatinosa Rolando after peripheral neurotomy. J Neurocytol 19: 329 – 337.

Chaudhry FA, Lehre KP, van Lookeren Campagne M, Ottersen OP, Danbolt NC and

Storm-Mathisen J (1995) Glutamate transporters in glial plasma membranes: highly differentiated localizations revealed by quantitative ultrastructural immunocytochemistry. Neuron 15: 711 – 720.

Chavis P and Westbrook G (2001) Integrins mediate functional pre-and postsynaptic maturation at a hippocampal synapse. Nature 411: 317 - 321.

Chen DH (1978) Qualitative and quantitative study of synaptic displacement in chromatolysed spinal motoneurons of the cat. J Comp Neurol 177: 635 – 664.

Cheney PD and Preston JB (1976a) Classification and response characteristics of muscle spindle afferents in the primate. J Neurophysiol 39: 1 – 8.

Cheney PD and Preston JB (1976b) Effects of fusimotor stimulation on dynamic and position sensitivities of spindle afferents in the primate. J Neurophysiol 39: 20 – 30.

Chiang RG and Govind CK (1986) Reorganization of synaptic ultrastructure at facilitated lobster neuromuscular terminals. J Neurocytol 15: 63 - 74.

Clements JD, Forsythe ID and Redman SJ (1987) Presynaptic inhibition of synaptic potentials evoked in cat spinal motoneurones by impulses in single group Ia axons. J Physiol (Lond) 383: 153 – 169.

Collins IWF, Mendell LM and Munson JB (1986) On the specificity of sensory reinnervation of cat skeletal muscle. J Physiol (Lond) 375: 587 – 609.

Cope TC, Bonasera SJ and Nichols TR (1994) Reinnervated muscles fail to produce stretch reflexes. J Neurophysiol 71: 817 - 820.

Cope TC and Clark BD (1993) Motor-unit recruitment in self-reinnervated muscle. J Neurophysiol 70: 1787 - 1796.

Decavel C and van den Pol AN (1990) GABA: a dominant neurotransmitter in the hypothalamus. J Comp Neurol 302: 1019 – 1037.

Crowe A and Matthews PBC (1964) The effects of stimulation of static and dynamic fusimotor fibers on the response to stretching of the primary endings of muscle spindle. J Physiol (Lond) 174: 109 – 131.

Devor M and Seltzer YY (1999) Pathophysiology of damaged nerves in relation to chronic pain. Textbook of Pain, 4th ed., Churchill Livingston, London, 129 – 164.

Di Giovanni S, De Biase A, Yakovlev A, Finn T, Beers J, Hoffman EP and Faden AI (2004) In vivo and in vitro characterization of novel neuronal plasticity factors identified following spinal cord injury. JBC Papers in Press, Manuscript M411975200.

Di Giovanni S, Faden AI, Yakovlev A, Duke-Cohan JS, Finn T, Thouin M, Knoblach S,

De Biase A, Bregman BS and Hoffman EP (2005) Neuronal plasticity after spinal cord injury: identification of a gene cluster driving neurite outgrowth. FASEB J Epub (1): 153 – 4.

Dittman JS and Regehr WG (1998) Calcium dependence and recovery kinetics of presynaptic depression at the climbing fiber to Purkinje cell synapse. J Neurosci 1: 6147 – 6162.

Edwards FR, Harrison PJ, Jack JJ and Kullmann DM (1989) Reduction by baclofen of monosynaptic EPSPs in lumbosacral motoneurones of the an aesthetized cat. J Physiol (Lond) 416: 539 – 556.

Erlander MG and Tobin AJ (1991) The structural and functional heterogeneity of glutamic acid decarboxylase: a review. Neurochem Res 16: 215 – 226.

Esclapez M, Tillakaratne NJK, Kaufman DL, Tobin AJ and Houser CR (1994) Comparative localization of two forms of glutamic acid decarboxylase and their mRNAs in rat brain supports the concept of functional differences between the forms. J Neurosci 14 (3): 1834 - 1855.

Feldblum S, Erlander MG and Tobin AJ (1995) Different distribution of GAD65 and GAD67 mRNA suggest that the two glutamate decarboxylases play different functional roles. J Neurosci Res 34: 689 –706.

Forgac M (2000) Structure, mechanism and regulation of the clathrin-coated vesicle and yeast vacuolar H+-ATPases. J Exp Biol 203: 71–80.

Fremeau RT, Troyer MD, Pahner I, Nygaard GO, Tran CH, Reimer RJ, Bellocchio EE, Fortin D, Storm-Mathisen J and Edwards RH (2001) The expression of vesicular glutamate transporters defines two classes of excitatory synapse. Neuron 31: 247–260.

Fremeau RT, Burman J, Qureshi T, Tran CH, Proctor J, Johnson J, Zhang H, Sulzer D, Copenhagen DR, Storm-Mathisen J, Reimer RJ, Chaudhry FA and Edwards RH (2002) The identification of vesicular glutamate transporter 3 suggests novel modes of signaling by glutamate. Proc Natl Acad Sci U. S. A. 99: 14488 – 14493.

Fremeau RT, Kam K, Qureshi T, Johnson J, Copenhagen DR, Storm-Mathisen J, ChaudhrFAy, Nicoll RA and Edwards RH (2004) Vesicular Glutamate Transporters 1 and 2 Target to Functionally Distinct Synaptic Release Sites. Science 304 (5678): 1815 - 1819.

Fremeau RT, Voglmaier S, Seal RP and Edwards RH (2004) VGLUTs define subsets of excitatory neurons and suggest novel roles for glutamate. Trends in Neurosci 27 (2): 98 – 103.

Gordon T (1987) Muscle plasticity during sprouting and reinnervation. Am Zool 27: 1055 - 1066.

Gordon T and Stein RB (1982) Time course and extent of recovery in reinnervated motor units of cat triceps surae muscles. J Physiol (Lond) 323: 307 - 323.

Govind CK and Chiang RG (1979) Correlation between presynaptic dense bodies and transmitter output at lobster neuromuscular terminals by serial section electron microscopy. Brain Res 161: 377 - 388.

Gras C, Herzog E, Bellenchi GC, Bernard V, Ravassard P, Pohl M, Gasnier B, Giros B and El Mestikawy S (2002) A third vesicular glutamate transporter expressed by cholinergic and serotoninergic neurons. J Neurosci 22: 5442 – 5451.

Gregory JE, Luff AR, Proske U (1982) Muscle receptors in the cross reinnervated soleus muscle of the cat. J Physiol (Lond) 331: 367 – 383.

Haftel VK, Bichler EK, Wang QB, Prather JF, Pinter MJ and Cope TC (2005) Central Suppression of Regenerated Proprioceptive Afferents. J Neurosci 25 (19): 4733 - 4742.

Haftel VK (1999) The effects of removal of homonymous afferent input on recruitment order and firing rate of medial gastrocnemius motoneurons in the decerabrate paralyzed cat [PhD]. Atlanta, Georgia: Emory University.

Hellgren J and Kellert JO (1989) A physiological study of the monosynaptic reflex responses of cat spinal motoneurons after partial lumbosacral deafferentation. Brain Res 488: 149 –162.

Hessler, NA, Shirke AM and Malinow R (1993) The probability of transmitter release at a mammalian central synapse. Nature 366: 569-572.

Hongo T, Jankowska E, Ohno T, Sasaki S, Yamashita M and Yoshida K (1983) The same interneurons mediate inhibition of dorsal spinocerebellar tract cells and lumbar motoneurons in the cat. J Physiol 342: 161 -180.

Houk JC, Rymer WZ, and Crago PE (1981) Dependence of dynamic response of spindle receptors on muscle length and velocity. J Neurophysiol 46: 143 – 166.

Hughes DI, Polgar E, Shehab SAS and Todd AJ (2004) Peripheral axotomy induces depletion of the vesicular glutamate transporter VGLUT1 in central terminals of myelinated afferent fibres in the rat spinal cord. Brain Res Issues 1-2 (1017): 69 - 76.

Hughes DI, Mackie M, Nagy GG, Riddell JS, Maxwell DJ, Szabo G, Erdelyi F, Veress G, Szucs P, Antal M, and Todd AJ (2005) P boutons in lamina IX of the rodent spinal cord express high levels of glutamic acid decarboxylase-65 and originate from cells in deep medial dorsal horn. PNAS 102 (25): 9038 – 9043.

Huyghues-Despointes CM, Cope TC and Nichols TR (2003) Intrinsic properties and reflex compensation in reinnervated triceps surae muscles of the cat: effect of activation

level. J Neurophysiol 90: 1537 - 1546.

Jankowska E and McCrea D (1983) Shared reflex pathways from Ib tendon organ afferents and Ia muscle spindle afferents in the cat. J Physiol 338: 99 - 111.

Jankowska E, McCrea D and Mackel R. (1981) Pattern of 'non-reciprocal' inhibition of motoneurones by impulses in group Ia muscle spindle afferents. J Physiol 316: 393 - 409.

Jankowska E and Roberts WJ (1972a) An electrophysiological demonstration of the axonal projections of single spinal interneurones in the cat. J Physiol 222: 597 - 622.

Jankowska E and Roberts WJ (1972b) Synaptic action of single interneurones mediating reciprocal Ia inhibition of motoneurones. J Physiol 222: 623 - 642.

Jimenez I, Rudomin P and Enriquez M (1991) Differential effects of (-)-baclofen on Ia and descending monosynaptic EPSPs. Exp Brain Res 85: 103 – 113.

Jin H, Wu H, Osterhaus G, Wei J, Davis K, Sha D, Floor E, Hsu C, Kopke RD and Wu J (2003) Demonstration of Functional Coupling between g-Aminobutyric Acid (GABA) Synthesis and Vesicular GABA Transport into Synaptic Vesicles. Proceedings of the National Academy of Sciences of the United States of America. 100 (7). 4293 - 4298.

Johnson RD and Munson JB (1991) Regenerating sprouts in axotomized cat muscle afferents express characteristic firing patterns to mechanical stimulation. J Neurophysiol 66: 2155 – 2158.

Johnson RG (1988) Accumulation of biological amines into chro-maffin granules: a model for hormone and neurotransmitter transport. Physiol Rev 68: 232 – 307.

Katarova Z, Szabo G, Mugnaini E and Greenspan RJ (1990) Molecular identification of the 62kd form of glutamic acid decarboxylase from the mouse. Eur J Neurosci 2: 190 - 202.

Kaufman DL, McGinnis JF, Krieeer NR and Tobin AJ (1986) Brain glutamate decarboxylase cloned h Xgt- 11: fusion protein produces γ-aminobutyric acid. Science 232: 1138 - l 140.

Kaufman DL, Houser CR and Tobin AJ (1991) Two forms of the gamma aminobutyric acid synthetic enzyme glutamate decarboxylase have distinctive intraneuronal distributions and cofactor interactions. J Neurochem 56: 720 – 723.

Koenig JH, Kosaka T and Ikeda K (1989) The relationship between the number of synaptic vesicles and the amount of transmitter released. J Neurosci 9 (6): 1937 – 1942.

Koerber HR, Mimics K, Brown PB and Mendell LM (1994) Central Sprouting and Functional Plasticity of Regenerated Primary Afferents. J. Neurosci 14 (6): 3655 - 3671.

Liu Y and Edwards RH (1997) The role of vesicular transport proteins in synaptic transmission and neural degeneration. Annu. Rev. Neurosci. 20: 125– 156.

Lee RY, Sawin ER, Chalfie M, Horvitz HR and Avery L (1999) EAT-4, a homolog of a mammalian sodium dependent inorganic phosphate cotransporter, is necessary for glutamatergic neurotransmission in Caenorhabditis elegans. J Neurosci 19: 159 – 167.

Lewin GR and McMahon SB (1991) Physiological properties of primary sensory neurons appropriately and inappropriately innervating skeletal muscle in adult rats. J Neurophysiol 66: 1218-1231.

Lnenicka GA, Atwood HL and Marin L (1986) Morphological transformation of synaptic terminals of a phasic motoneuron by long-term tonic stimulation. J Neurosci 6: 2252 - 2258.

Mackie M, Hughes DI, Maxwell DJ, Tillakaratneb JK and Todd AJ (2003) Distribution and colocalisation of glutamate decarboxylase isoforms in the rat spinal cord. Neuroscience 119: 461– 472.

Matthews PBC (1963) The response of de-efferented muscle spindle receptors to stretching at different velocities. J Physiol (Lond) 168: 660 – 678.

McCloskey DI (1978) Kinesthetic sensibility. Physiol Rev 58: 763– 820.

Mendell LM, Taylor JS, Johnson RD and Munson JB (1995) Rescue of motoneuron and muscle afferent function in cats by regeneration into skin: II. Ia-Motoneuron synapse. J Neurophysiol 73. 662 – 673.

Moore KA, Kohno T, Karchewski LA, Scholz J, Baba H and Woolf CJ. (2002) Partial peripheral nerve injury promotes a selective loss of GABAergic inhibition in the superficial dorsal horn of the spinal cord. J Neurosci 22: 6724 - 31.

Nam HK, Choi KS, Park KP and Bae YC (2002) Quantitative and ultrastructural analysis of afferent terminals from tooth pulp in the trigeminal principal sensory nucleus. Korean J Anat 35 (5): 439 - 452.

Navarrete R, Shahani U and Vrbova G (1990) Long-lasting modification of reflexes after neonatal nerve injury in the rat. J Neurol Sci 96: 257 – 265.

Ni B, Rosteck PR Jr, Nadi NS and Paul SM (1994) Proc Natl Acad Sci USA 91: 5607 – 5611.

Ni B, Wu X, Yan G, Wang J and Paul SM (1995) Regional expression and cellular localization of the Na+-dependent inorganic phosphate cotransporter of rat brain. J Neurosci 15: 5789 – 5799.

Nielsen J, Crone C and Hultborn H (1993) H-reflexes are smaller in dancers from the

Royal Danish Ballet than in well-trained athletes. Eur J Appl Physiol Occup Physiol 66: 116 – 121.

Miyazaki T, Fukaya M, Shimizu H and Watanabe M (2003) Subtype switching of vesicular glutamate transporters at parallel fibre–Purkinje cell synapses in developing mouse cerebellum. Eur J Neurosci 17: 2563–2572.

Otis S (2001) Vesicular glutamate transporters in cognito: Minireview. Neuron (29): 11 – 14.

Perez, MA and Nielsen JB (2004) Reduced Soleus H-Reflex After Training of a Task Involving Co-Contraction of Antagonistic Ankle Muscles. Program no. 656.16. Abstract Viewer/Itinerary Planner. Society for Neuroscience, Washington, DC.

Pierce PP and Mendell LM (1993) la Bouton Ultrastructure: Scaling and Positional Factors. J Neurosci 13 (11): 4759.

Prochazka A, Westerman RA and Ziccone SP (1976) Discharge of single hindlimb afferents in the freely moving cat. J Neurophysiol 39: 1090 - 1104.

Propst JW and Ko CP (1987) Correlations between active zone ultrastructure and synaptic function studied with freeze-fracture of physiologically identified neuromuscular junctions. J Neurosci 7: 3654 – 3664.

Rosenmund C, Clements JD and Westbrook GL (1993) Nonuniform probability of glutamate release at a hippocampal synapse. Science 262: 754 – 757.

Rothstein JD and Tabakoff B (1984) Alteration of striatal glutamate release after glutamine synthetase inhibition. J Neurochem 43: 1438 – 1446.

Rudomin P and Schmidt RF (1999) Presynaptic inhibition in the vertebrate spinal cord revisited. Exp Brain Res 129: 1 – 37.

Schafer MK, Varoqui H, Defamie N, WeiheDagger E and Erickson JD (2002) Molecular cloning and functional identification of mouse vesicular glutamate transporter 3 and its expression in subsets of novel excitatory neurons. J Biol Chem 277: 50734 - 50748.

Schuldiner S, Shirvan A and Linial M (1995) Vesicular neurotransmitter transporters: From bacteria to humans. Physiol Rev 75: 369 – 392.

Takamori S, Rhee JS, Rosenmund C and Jahn R (2000) Identification of a vesicular glutamate transporter that defines a glutamatergic phenotype in neurons. Nature 407: 189 – 194.

Todd AJ, Hughes DI, Polgar E, Nagy GG, Mackie M, Ottersen OP and Maxwell DJ (2003) The expression of vesicular glutamate transporters VGLUT1 and VGLUT2 in neurochemically defined axonal populations in the rat spinal cord with emphasis on the

dorsal horn. Euro J Neurosci 17: 13–27.

Todd AJ and Maxwell DJ (2000) GABA in the mammalian spinal cord. In: GABA in the nervous system: the view at fifty years (Martin DL, Olsen RW, eds). Philadelphia, PA, USA: Lippincott, Williams and Wilkins. 439 – 457.

Tse FW, Marin L, Jahromi SS and Atwood HL (1991) Variation in terminal morphology and presynaptic inhibition at crustacean neuromuscular junctions. J Comp Neurol 304: 135 - 1 46.

Tillakaratne NJK, De Leon RD, Hoang TX, Roy RR, Edgerton VR and Tobin AJ (2002) Use-dependent modulation of inhibitory capacity in the feline lumbar spinal cord. J Neurosci 22: 3130 - 3143.

Valero-Cabre A and Navarro X (2001) H reflex restitution and facilitation after different types of peripheral nerve injury and repair. Brain Res 919: 302 – 312.

Valero-Cabré A and Navarro X (2002) Functional impact of axonal misdirection after peripheral nerve injuries followed by graft or tube repair. J Neurotrauma 19: 1475 - 1485.

Van Dyke RW (1988) Proton pump-generated electrochemical gradients in rat liver multivesicular bodies: Quantitation and effects of chloride. J Biol Chem 263: 2603 - 2611.

Varoqui H, Schafer MK, Zhu H, Weihe E and Erickson JD (2002) Identification of the differentiation-associated Naþ/PI transporter as a novel vesicular glutamate transporter expressed in a distinct set of glutamatergic synapses. J Neurosci 22: 142 – 155.

Wakisaka S, Kajander KC and Bennett GJ (1991) Increased neuropeptide Y (NPY)-like immunoreactivity in rat sensory neurons following peripheral axotomy. Neurosci Lett 124: 200 – 203.

Wakisaka S, Kajander KC and Bennett GJ (1992) Effects of peripheral nerve injuries and tissue inflammation on the levels of neuropeptide Y-like immunoreactivity in rat primary afferent neurons. Brain Res 598: 349 – 352.

Wall PD and Devor M (1981) The effect of peripheral nerve injury on dorsal root potentials and on transmission of afferent signals into the spinal cord. Brain Res 209: 95 – 111.

Wall PD and Lidieth M (1997) Five sources of a dorsal root potential: Their interactions and origins in the superficial dorsal horn, J Neurophysiol 78 (2): 860 - 871.

Waller A (1850) Experiments on the section of glossopharyngeal and hypoglossal nerves of the frog and observations of the alternatives produced thereby in the structure of their primitive fibers. Philos Trans R Soc Lond Biol 140: 423.

Watson AHD and Bazzaz AA (2001) GABA and glycine-like immunoreactivity at axoaxonic synapses on 1a muscle afferent terminals in the spinal cord of the rat. J Comp Neurol 433 (3): 335 – 348.